



# Pathway Analysis Report

This report contains the pathway analysis results for the submitted sample ". Analysis was performed against Reactome version 95 on 10/12/2025. The web link to these results is:

<https://reactome.org/PathwayBrowser/#/ANALYSIS=MjAyNTEyMTAxOTA4MDNfMjM3NQ%3D%3D>

Please keep in mind that analysis results are temporarily stored on our server. The storage period depends on usage of the service but is at least 7 days. As a result, please note that this URL is only valid for a limited time period and it might have expired.

# Table of Contents

1. Introduction
2. Properties
3. Genome-wide overview
4. Most significant pathways
5. Pathways details
6. Identifiers found
7. Identifiers not found

# 1. Introduction

Reactome is a curated database of pathways and reactions in human biology. Reactions can be considered as pathway 'steps'. Reactome defines a 'reaction' as any event in biology that changes the state of a biological molecule. Binding, activation, translocation, degradation and classical biochemical events involving a catalyst are all reactions. Information in the database is authored by expert biologists, entered and maintained by Reactome's team of curators and editorial staff. Reactome content frequently cross-references other resources e.g. NCBI, Ensembl, UniProt, KEGG (Gene and Compound), ChEBI, PubMed and GO. Orthologous reactions inferred from annotation for *Homo sapiens* are available for 14 non-human species including mouse, rat, chicken, puffer fish, worm, fly and yeast. Pathways are represented by simple diagrams following an SBGN-like format.

Reactome's annotated data describe reactions possible if all annotated proteins and small molecules were present and active simultaneously in a cell. By overlaying an experimental dataset on these annotations, a user can perform a pathway over-representation analysis. By overlaying quantitative expression data or time series, a user can visualize the extent of change in affected pathways and its progression. A binomial test is used to calculate the probability shown for each result, and the p-values are corrected for the multiple testing (Benjamini–Hochberg procedure) that arises from evaluating the submitted list of identifiers against every pathway.

To learn more about our Pathway Analysis, please have a look at our relevant publications:

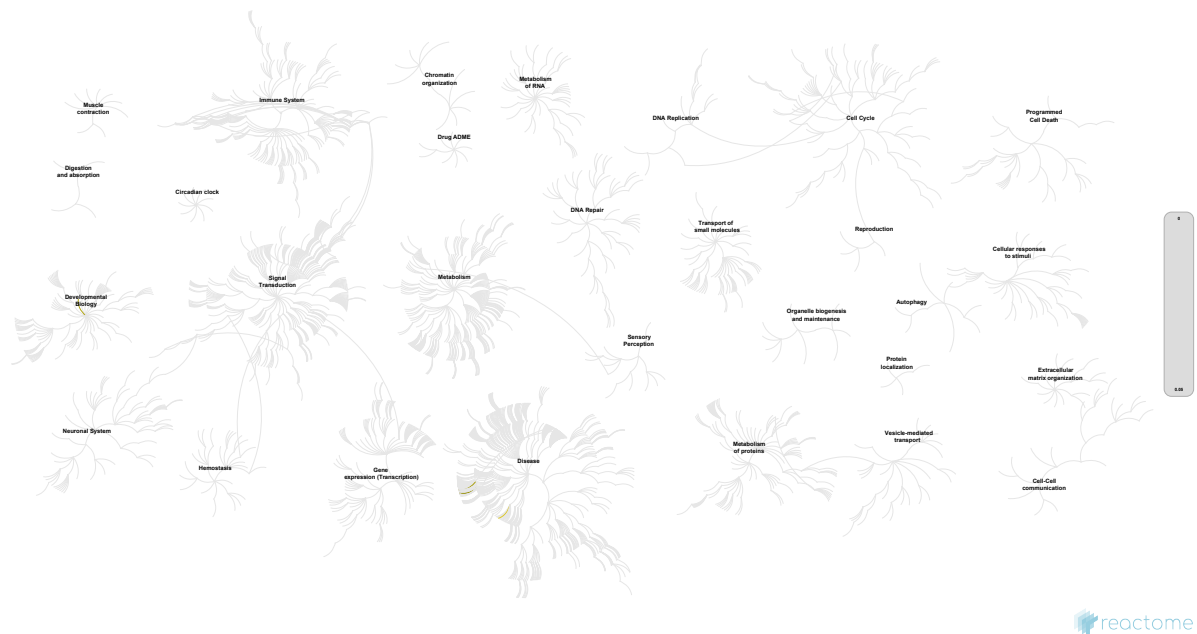
Fabregat A, Sidiropoulos K, Garapati P, Gillespie M, Hausmann K, Haw R, ... D'Eustachio P (2016). The reactome pathway knowledgebase. *Nucleic Acids Research*, 44(D1), D481–D487. <https://doi.org/10.1093/nar/gkv1351>. 

Fabregat A, Sidiropoulos K, Viteri G, Forner O, Marin-Garcia P, Arnau V, ... Hermjakob H (2017). Reactome pathway analysis: a high-performance in-memory approach. *BMC Bioinformatics*, 18. 

## 2. Properties

- This is an **overrepresentation** analysis: A statistical (hypergeometric distribution) test that determines whether certain Reactome pathways are over-represented (enriched) in the submitted data. It answers the question 'Does my list contain more proteins for pathway X than would be expected by chance?' This test produces a probability score, which is corrected for false discovery rate using the Benjamani-Hochberg method. ↗
- 574 out of 1462 identifiers in the sample were found in Reactome, where 2094 pathways were hit by at least one of them.
- All non-human identifiers have been converted to their human equivalent. ↗
- IntAct interactors were included to increase the analysis background. This greatly increases the size of Reactome pathways, which maximises the chances of matching your submitted identifiers to the expanded pathway, but will include interactors that have not undergone manual curation by Reactome and may include interactors that have no biological significance, or unexplained relevance.
- This report is filtered to show only results for species 'Homo sapiens' and resource 'all resources'.
- The unique ID for this analysis (token) is MjAyNTEyMTAxOTA4MDNfMjM3NQ%3D%3D. This ID is valid for at least 7 days in Reactome's server. Use it to access Reactome services with your data.

### 3. Genome-wide overview



This figure shows a genome-wide overview of the results of your pathway analysis. Reactome pathways are arranged in a hierarchy. The center of each of the circular "bursts" is the root of one top-level pathway, for example "DNA Repair". Each step away from the center represents the next level lower in the pathway hierarchy. The color code denotes over-representation of that pathway in your input dataset. Light grey signifies pathways which are not significantly over-represented.

## 4. Most significant pathways

The following table shows the 25 most relevant pathways sorted by p-value.

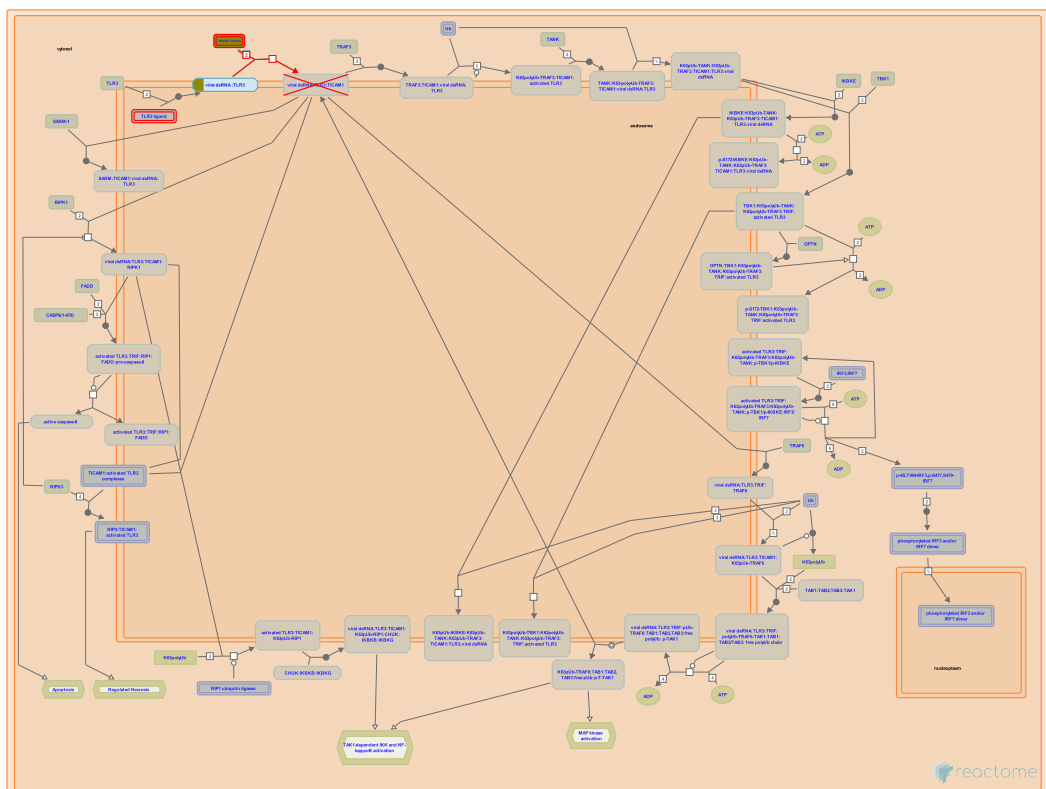
Pathway name	Entities				Reactions	
	found	ratio	p-value	FDR*	found	ratio
TICAM1 deficiency - HSE	2 / 2	8.06e-05	0.013	1	1 / 1	6.30e-05
LGI-ADAM interactions	4 / 14	5.64e-04	0.034	1	4 / 5	3.15e-04
Defective B3GALT6 causes EDSP2 and SEMDJL1	5 / 21	8.46e-04	0.037	1	1 / 1	6.30e-05
Glycogen storage disease type IV (GBE1)	2 / 4	1.61e-04	0.047	1	1 / 1	6.30e-05
JNK (c-Jun kinases) phosphorylation and activation mediated by activated human TAK1	5 / 26	0.001	0.076	1	1 / 3	1.89e-04
Developmental Lineage of Pancreatic Acinar Cells	12 / 87	0.004	0.078	1	3 / 3	1.89e-04
Drug resistance of KIT mutants	1 / 1	4.03e-05	0.082	1	7 / 7	4.41e-04
KIT mutants bind TKIs	1 / 1	4.03e-05	0.082	1	3 / 3	1.89e-04
Imatinib-resistant KIT mutants	1 / 1	4.03e-05	0.082	1	1 / 1	6.30e-05
TLR3 deficiency - HSE	1 / 1	4.03e-05	0.082	1	1 / 1	6.30e-05
Sorafenib-resistant KIT mutants	1 / 1	4.03e-05	0.082	1	1 / 1	6.30e-05
Regorafenib-resistant KIT mutants	1 / 1	4.03e-05	0.082	1	1 / 1	6.30e-05
Masitinib-resistant KIT mutants	1 / 1	4.03e-05	0.082	1	1 / 1	6.30e-05
Nilotinib-resistant KIT mutants	1 / 1	4.03e-05	0.082	1	1 / 1	6.30e-05
Sunitinib-resistant KIT mutants	1 / 1	4.03e-05	0.082	1	1 / 1	6.30e-05
Dasatinib-resistant KIT mutants	1 / 1	4.03e-05	0.082	1	1 / 1	6.30e-05
GABA synthesis	2 / 6	2.42e-04	0.095	1	2 / 2	1.26e-04
Defective B4GALT7 causes EDS, progeroid type	4 / 21	8.46e-04	0.109	1	1 / 1	6.30e-05
Defective B3GAT3 causes JDSSDHD	4 / 22	8.86e-04	0.124	1	1 / 1	6.30e-05
MAP2K and MAPK activation	7 / 51	0.002	0.154	1	10 / 12	7.56e-04
Defective SLCO1B1 causes hyperbilirubinemia, Rotor type (HBLRR)	1 / 2	8.06e-05	0.158	1	1 / 1	6.30e-05
Signaling by high-kinase activity BRAF mutants	6 / 44	0.002	0.182	1	4 / 6	3.78e-04
Defective CHST3 causes SEDCJD	2 / 9	3.62e-04	0.182	1	1 / 1	6.30e-05
Defective CHST14 causes EDS, musculocontractural type	2 / 9	3.62e-04	0.182	1	1 / 1	6.30e-05
activated TAK1 mediates p38 MAPK activation	4 / 27	0.001	0.205	1	1 / 5	3.15e-04

\* False Discovery Rate

## 5. Pathways details

For every pathway of the most significant pathways, we present its diagram, as well as a short summary, its bibliography and the list of inputs found in it.

### 1. TICAM1 deficiency - HSE (R-HSA-5602566)



**Diseases:** primary immunodeficiency disease.

Inborn errors of interferon immunity due to defects in toll like receptor 3 (TLR3)-mediated signaling underlie pathogenesis of herpes simplex virus type 1 (HSV1) encephalitis (HSE) in some children (Netea MG et al. 2012). Autosomal dominant (AD) and recessive (AR) deficiencies of (TIR) domain-containing adaptor inducing IFN-beta (TRIF or TICAM1) are also associated with impaired IFN production and predisposition to HSE in the course of primary infection by HSV1 (Sancho-Shimizu V et al. 2011).

### References

Sancho-Shimizu V, Pérez de Diego R, Lorenzo L, Halwani R, Alangari A, Israelsson E, ... Casanova JL (2011). Herpes simplex encephalitis in children with autosomal recessive and dominant TRIF deficiency. *J. Clin. Invest.*, 121, 4889-902. [View](#)

### Edit history

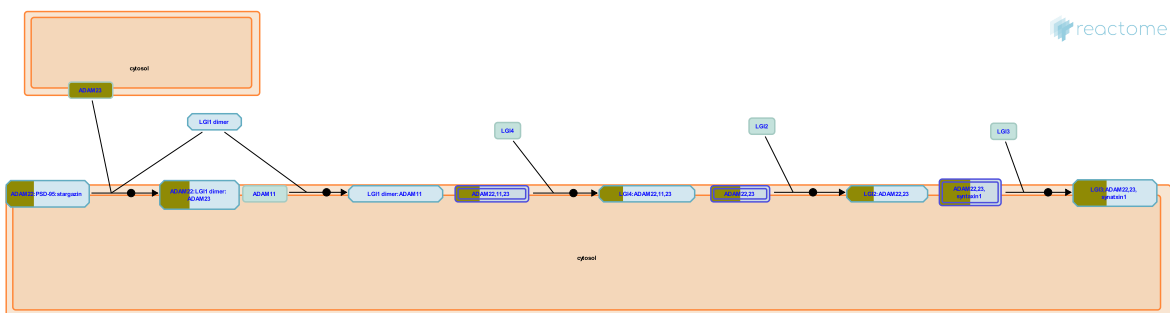
Date	Action	Author
2014-05-21	Authored	Shamovsky V
2014-06-24	Created	Shamovsky V
2014-09-06	Reviewed	D'Eustachio P

Date	Action	Author
2015-02-10	Edited	Shamovsky V
2015-02-15	Reviewed	McDonald DR
2023-03-08	Modified	Matthews L

**2 submitted entities found in this pathway, mapping to 2 Reactome entities**

Input	UniProt Id	Input	UniProt Id
PLIN3	Q8IUC6	TLR3	O15455

## 2. LGI-ADAM interactions (R-HSA-5682910)



**Cellular compartments:** extracellular region.

Synapse formation and maturation require multiple interactions between presynaptic and postsynaptic neurons. These interactions are mediated by a diverse set of synaptogenic proteins (Kegel et al. 2013, Siddiqui & Craig 2011). Initial synapse formation needs both the binding of secreted proteins to presynaptic and postsynaptic receptors, and the direct binding between presynaptic and postsynaptic transmembrane proteins. One class of molecules that plays an important role in cellular interactions in nervous system development and function is the leucine-rich glioma inactivated (LGI) protein family. These are secreted synaptogenic proteins consisting of an LRR (leucine-rich repeat) domain and a epilepsy-associated or EPTP (epitempin) domain (Gu et al. 2002). Both protein domains are generally involved in protein-protein interactions. Genetic and biochemical evidence suggests that the mechanism of action of LGI proteins involves binding to a subset of cell surface receptors belonging to the ADAM (a disintegrin and metalloproteinase) family, i.e. ADAM11, ADAM22 and ADAM23. These interactions play crucial role in the development and function of the vertebrate nervous system mainly mediating synaptic transmission and myelination (Kegel et al. 2013, Novak 2004, Seals & Courtneidge 2003).

## References

Kegel L, Aunin E, Meijer D & Bermingham JR (2013). LGI proteins in the nervous system. ASN Neuro, 5, 167-81. [View](#)

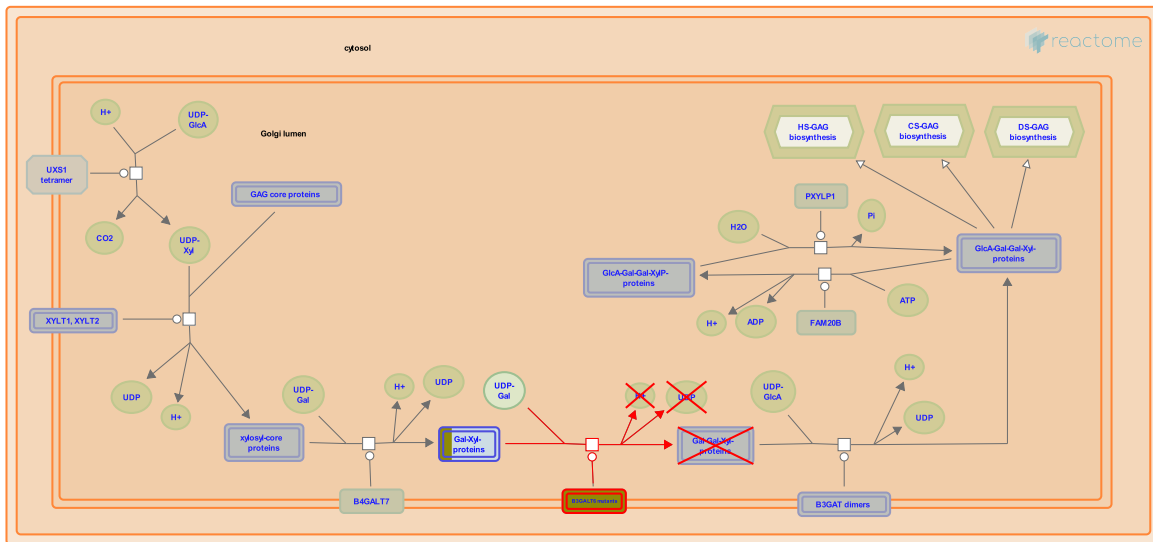
## Edit history

Date	Action	Author
2015-03-11	Edited	Garapati P V
2015-03-11	Authored	Garapati P V
2015-03-11	Created	Garapati P V
2015-04-20	Reviewed	Meijer D
2025-11-15	Modified	Weiser JD

4 submitted entities found in this pathway, mapping to 4 Reactome entities

Input	UniProt Id	Input	UniProt Id
ADAM23	O75077	CACNG4	Q9UBN1
CACNG8	Q8WXS5	STX1B	P61266

### 3. Defective B3GALT6 causes EDSP2 and SEMDJL1 (R-HSA-4420332)



**Diseases:** Ehlers-Danlos syndrome, spondyloepimetaphyseal dysplasia.

The biosynthesis of dermatan sulfate/chondroitin sulfate and heparin/heparan sulfate glycosaminoglycans (GAGs) starts with the formation of a tetrasaccharide linker sequence attached to the core protein. Beta-1,3-galactosyltransferase 6 (B3GALT6) is one of the critical enzymes involved in the formation of this linker sequence. Defects in B3GALT6 cause Ehlers-Danlos syndrome progeroid type 2 (EDSP2; MIM:615349), a severe disorder resulting in a broad spectrum of skeletal, connective tissue and wound healing problems. Defects in B3GALT6 can also cause spondyloepimetaphyseal dysplasia with joint laxity type 1 (SEMDJL1; MIM:271640), characterised by spinal deformity and lax joints, especially of the hands and respiratory compromise resulting in early death (Nakajima et al. 2013, Malfait et al. 2013).

## References

- Malfait F, Kariminejad A, Van Damme T, Gauche C, Syx D, Merhi-Soussi F, ... De Paepe A (2013). Defective Initiation of Glycosaminoglycan Synthesis due to B3GALT6 Mutations Causes a Pleiotropic Ehlers-Danlos Syndrome-like Connective Tissue Disorder. *Am. J. Hum. Genet.*. ↗
- Nakajima M, Mizumoto S, Miyake N, Kogawa R, Iida A, Ito H, ... Ikegawa S (2013). Mutations in B3GALT6, which Encodes a Glycosaminoglycan Linker Region Enzyme, Cause a Spectrum of Skeletal and Connective Tissue Disorders. *Am. J. Hum. Genet.*. ↗

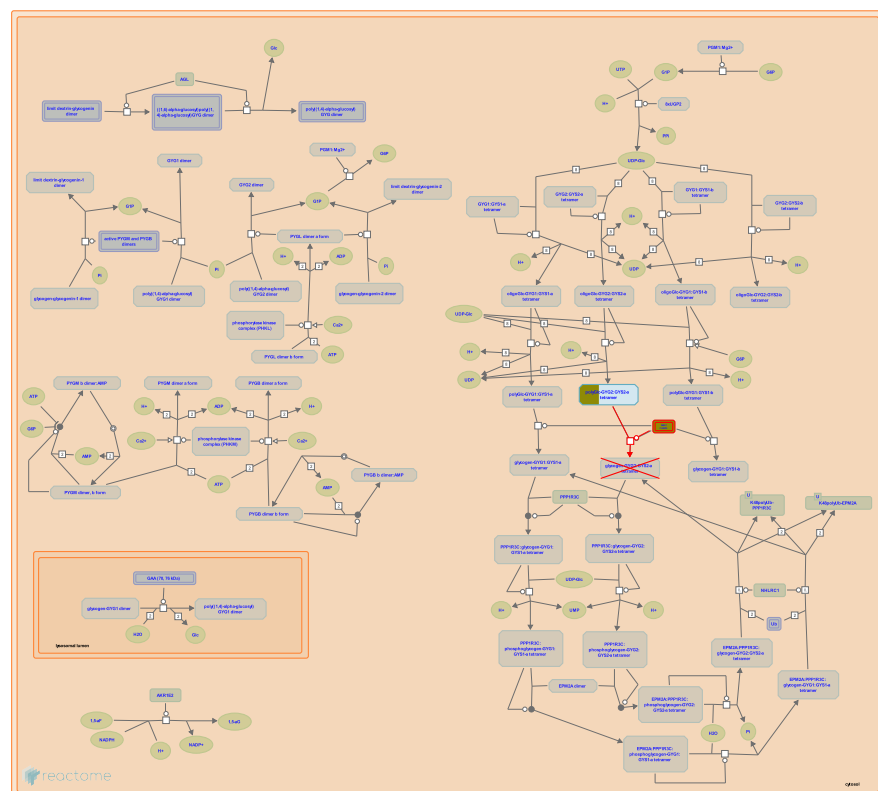
## Edit history

Date	Action	Author
2013-09-03	Edited	Jassal B
2013-09-03	Authored	Jassal B
2013-09-03	Created	Jassal B
2014-07-09	Reviewed	Spillmann D
2025-06-02	Modified	Stephan R

5 submitted entities found in this pathway, mapping to 5 Reactome entities

Input	UniProt Id	Input	UniProt Id	Input	UniProt Id
B3GALT6	Q96L58	BGN	P21810	CSPG5	O95196
GPC2	Q8N158	GPC5	P78333		

#### 4. Glycogen storage disease type IV (GBE1) ([R-HSA-3878781](#))



**Diseases:** glycogen storage disease IV.

Normally, cytosolic glycogen branching enzyme (GBE1) associated with glycogen granules transfers terminal alpha(1,4) glucose blocks to form alpha(1,6) branches on growing glycogen molecules of both liver and muscle types. In the absence of GBE1 activity, abnormal amylopectin-like glycogen with longer alpha(1,4) chains and fewer branch points forms in all tissues where glycogen is normally found. Presentation of the disease is clinically heterogeneous: missense and nonsense mutations associated with little or no enzyme activity can lead to progressive liver disease or neuromuscular disease (Bao et al. 1996; Bruno et al. 2004).

#### References

- Bruno C, van Diggelen OP, Cassandrini D, Gimpelev M, Giuffrè B, Donati MA, ... Minetti C (2004). Clinical and genetic heterogeneity of branching enzyme deficiency (glycogenosis type IV). *Neurology*, 63, 1053-8. [\[CrossRef\]](#)
- Bao Y, Kishnani P, Wu JY & Chen Y-T (1996). Hepatic and neuromuscular forms of glycogen storage disease type IV caused by mutations in the same glycogen-branched enzyme gene. *J Clin Invest*, 97, 941-8. [\[CrossRef\]](#)

#### Edit history

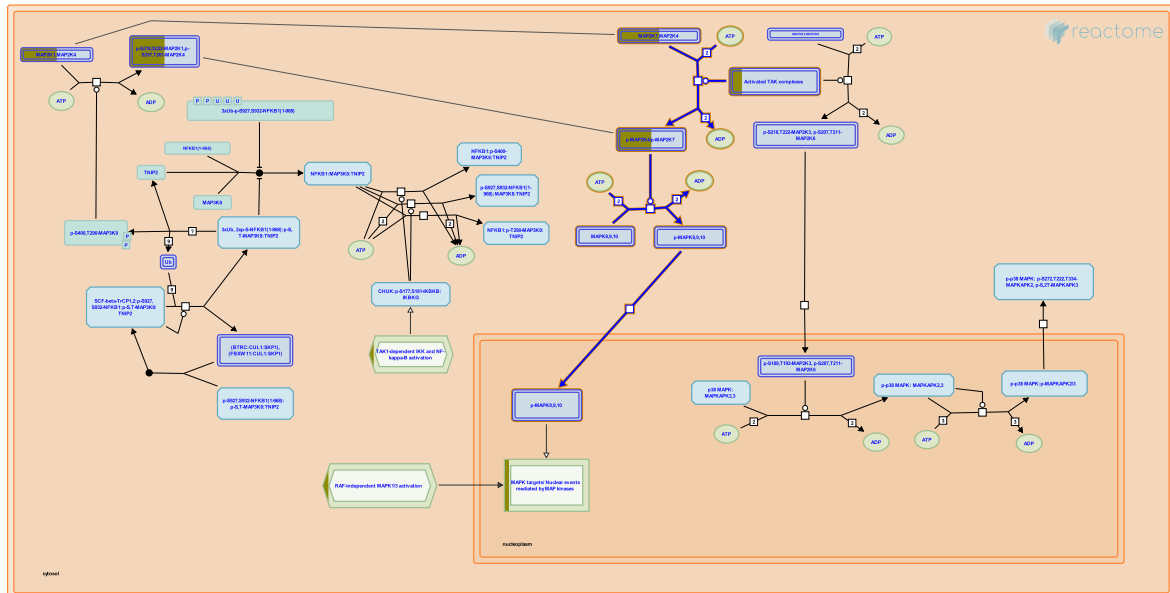
Date	Action	Author
2013-07-12	Created	D'Eustachio P
2013-07-19	Edited	D'Eustachio P
2013-07-19	Authored	D'Eustachio P
2015-08-17	Reviewed	Jassal B

Date	Action	Author
2023-10-12	Modified	Weiser JD

**2 submitted entities found in this pathway, mapping to 2 Reactome entities**

Input	UniProt Id	Input	UniProt Id
GBE1	Q04446	GYG2	O15488

## 5. JNK (c-Jun kinases) phosphorylation and activation mediated by activated human TAK1 (R-HSA-450321)



**Cellular compartments:** cytosol, nucleoplasm.

C-Jun NH<sub>2</sub> terminal kinases (JNKs) are an evolutionarily conserved family of serine/threonine protein kinases, that belong to mitogen activated protein kinase family (MAPKs - also known as stress-activated protein kinases, SAPKs). The JNK pathway is activated by heat shock, or inflammatory cytokines, or UV radiation.

The JNKs are encoded by at least three genes: JNK1/SAPK-gamma, JNK2/SAPK-alpha and JNK3/SAPK-beta. The first two are ubiquitously expressed, whereas the JNK3 protein is found mainly in brain and to a lesser extent in heart and testes. As a result of alternative gene splicing all cells express distinct active forms of JNK from 46 to 55 kDa in size. Sequence alignment of these different products shows homologies of >80%. In spite of this similarity, the multiple JNK isoforms differ in their ability to bind and phosphorylate different target proteins, thus leading to the distinctive cellular processes: induction of apoptosis, or enhancement of cell survival, or proliferation.

Activation of JNKs is mediated by activated TAK1 which phosphorylates two dual specificity enzymes MKK4 (MAPK kinase 4) and MKK7(MAPK kinase 7).

### References

- Thiebes A, Wolter S, Mushinski JF, Hoffmann E, Dittrich-Breiholz O, Graue N, ... Kracht M (2005). Simultaneous blockade of NFκB, JNK, and p38 MAPK by a kinase-inactive mutant of the protein kinase TAK1 sensitizes cells to apoptosis and affects a distinct spectrum of tumor necrosis factor [corrected] target genes. *J Biol Chem*, 280, 27728-41. [🔗](#)
- Wang C, Deng L, Hong M, Akkaraju GR, Inoue J & Chen ZJ (2001). TAK1 is a ubiquitin-dependent kinase of MKK and IKK. *Nature*, 412, 346-51. [🔗](#)
- Li JK, Nie L, Zhao YP, Zhang YQ, Wang X, Wang SS, ... Cheng L (2016). IL-17 mediates inflammatory reactions via p38/c-Fos and JNK/c-Jun activation in an AP-1-dependent manner in human nucleus pulposus cells. *J Transl Med*, 14, 77. [🔗](#)

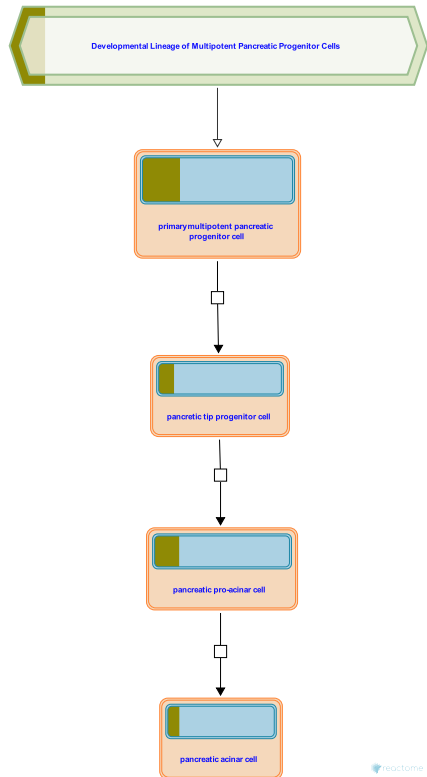
### Edit history

Date	Action	Author
2009-12-16	Authored	Shamovsky V
2009-12-16	Created	Shamovsky V
2010-02-28	Edited	Shamovsky V
2010-02-28	Reviewed	Gillespie ME

### 5 submitted entities found in this pathway, mapping to 5 Reactome entities

Input	UniProt Id	Input	UniProt Id	Input	UniProt Id
IRAK1	P51617	NEK4	P45985	RIPK2	O43353
TAB1	Q15750	TAB2	Q9NYJ8		

## 6. Developmental Lineage of Pancreatic Acinar Cells ([R-HSA-9925561](#))



The exocrine pancreas, which comprises more than 95% of the pancreas mass, consists of lobules formed by tubuloacinar glands that are built by two cell types: acinar cells and ductal cells. A third, centroacinar cells type has been identified in murine studies, but their existence and functional role is under debate. Acinar cells are large pyramidal secretory epithelial cells, with apical-basal polarization, that surround the lumen of the acinus. Acinar cells have prominent endoplasmic reticulum and Golgi networks, and their cytoplasm contains a large number of secretory zymogen granules, filled with various digestive enzymes, that are clustered in the vicinity of the apical surface. At the surface of the lumen, acinar cells are attached to each other by apical tight junctions, while their basal surfaces are associated with the basal lamina. For overview, please refer to Liggitt and Dintzis, "Pancreas", 241-250. For review, please refer to Tritschler et al. 2017.

Pancreatic acinar cells originate from definitive endoderm cells that form during gastrulation, and then undergo patterning along anterior/posterior, dorsal/ventral, and median/lateral axes, producing, among other embryonal cell types, endoderm cells of dorsal and ventral foregut, which, after transitioning through an intermediary duodeno-pancreatic endoderm cell state for dorsal foregut endoderm and possibly a hepato-pancreatic or pancreato-biliary intermediary state for ventral foregut endoderm, give rise to multipotent pancreatic progenitor cells (MPCs) that form dorsal and ventral pancreatic buds (Yu et al. 2019, reviewed in Jennings et al. 2015). Developing pancreas undergoes branching morphogenesis, which results in the apical-basal polarity that is critical for establishing the acinar-ductal functional unit (Darrigrand et al. 2024). Both dorsal and ventral MPCs located at the tips of the developing, branching pancreas, start committing to the acinar cell fate from Carnegie stage 19 (45-47 days post conception) of human embryonic development and around embryonic day E12 during mouse development, initially becoming distinct tip progenitors, and then pro-acinar and acinar cells (Yu et al. 2019, reviewed in Jennings et al. 2015).

## References

Jennings RE, Berry AA, Strutt JP, Gerrard DT & Hanley NA (2015). Human pancreas development. Development, 142, 3126-37. [🔗](#)

Liggitt D & Dintzis SM (2018). *Pancreas*, "Pancreas", in "Comparative Anatomy and Histology. A Mouse, Rat, and Human Atlas.", edited by Treuting, Dintzis and Montine., pp. 241-250.

Tritschler S, Theis FJ, Lickert H & Böttcher A (2017). Systematic single-cell analysis provides new insights into heterogeneity and plasticity of the pancreas. Mol Metab, 6, 974-990. [🔗](#)

Yu XX, Qiu WL, Yang L, Zhang Y, He MY, Li LC & Xu CR (2019). Defining multistep cell fate decision pathways during pancreatic development at single-cell resolution. EMBO J, 38. [🔗](#)

Darrigrand JF, Salowka A, Torres-Cano A, Tapia-Rojo R, Zhu T, Garcia-Manyes S & Spagnoli FM (2024). Acinar-ductal cell rearrangement drives branching morphogenesis of the murine pancreas in an IGF/PI3K-dependent manner. Dev Cell, 59, 326-338.e5. [🔗](#)

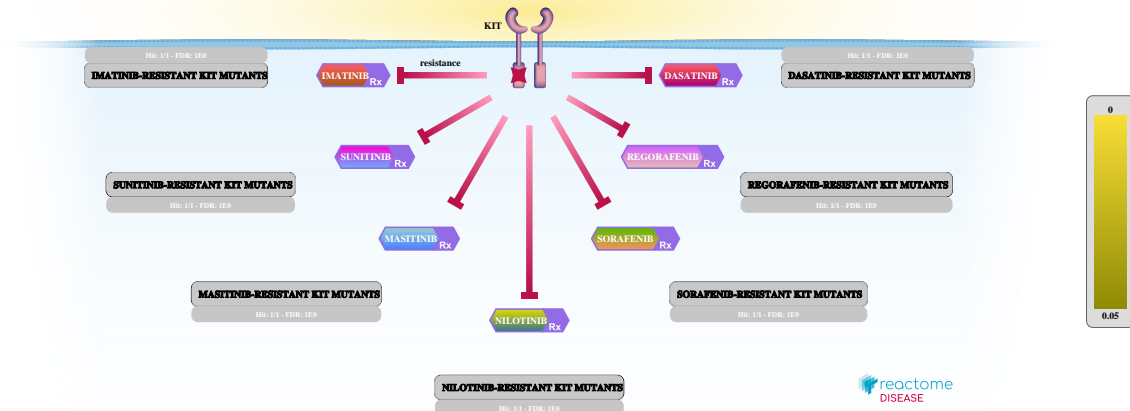
## Edit history

Date	Action	Author
2024-10-17	Authored	Orlic-Milacic M
2024-10-17	Created	Orlic-Milacic M
2024-10-30	Reviewed	Li NT
2024-11-04	Edited	Orlic-Milacic M
2025-01-29	Modified	Orlic-Milacic M
2025-01-29	Reviewed	Li NT

## 7 submitted entities found in this pathway, mapping to 12 Reactome entities

Input	UniProt Id	Input	UniProt Id	Input	UniProt Id
BHLHA15	Q7RTS1	CPA2	P48052	CTRC	Q99895
ONECUT1	Q9UBC0	PDX1	P52945		
Input	Ensembl Id	Input	Ensembl Id	Input	Ensembl Id
AMY2B	ENST00000361355	ANPEP	ENST00000300060	BHLHA15	ENST00000609256
CPA2	ENST00000222481	CTRC	ENST00000375949	ONECUT1	ENST00000305901
PDX1	ENST00000381033				

## 7. Drug resistance of KIT mutants (R-HSA-9669937)



**Diseases:** cancer.

Activating mutations in the juxtamembrane domain of KIT are common in some cancers, including gastrointestinal stromal tumors, melanoma and acute myeloid leukemia (reviewed in Roskoski, 2018). These mutations are sensitive to inhibition with imatinib, which in 2001 was the first tyrosine kinase inhibitor approved for treatment of cancer (Demetri et al, 2002; Corless et al, 2011; reviewed in Zitvogel, 2016). Although highly successful in prolonging survival, imatinib-resistance develops in most patients due to appearance of secondary mutations, often in the ATP-binding pocket or in the activation loop of the kinase domain (Gajiwala et al, 2008; Serrano et al, 2019; reviewed in Roskoski, 2018; Napolitano and Vincenzi, 2019)

## References

- Roskoski R (2018). The role of small molecule Kit protein-tyrosine kinase inhibitors in the treatment of neoplastic disorders. *Pharmacol. Res.*, 133, 35-52. [🔗](#)
- Demetri GD, von Mehren M, Blanke CD, Van den Abbeele AD, Eisenberg B, Roberts PJ, ... Joensuu H (2002). Efficacy and safety of imatinib mesylate in advanced gastrointestinal stromal tumors. *N. Engl. J. Med.*, 347, 472-80. [🔗](#)
- Corless CL, Barnett CM & Heinrich MC (2011). Gastrointestinal stromal tumours: origin and molecular oncology. *Nat. Rev. Cancer*, 11, 865-78. [🔗](#)
- Zitvogel L, Rusakiewicz S, Routy B, Ayyoub M & Kroemer G (2016). Immunological off-target effects of imatinib. *Nat Rev Clin Oncol*, 13, 431-46. [🔗](#)
- Gajiwala KS, Wu JC, Christensen J, Deshmukh GD, Diehl W, DiNitto JP, ... Demetri GD (2009). KIT kinase mutants show unique mechanisms of drug resistance to imatinib and sunitinib in gastrointestinal stromal tumor patients. *Proc. Natl. Acad. Sci. U.S.A.*, 106, 1542-7. [🔗](#)

## Edit history

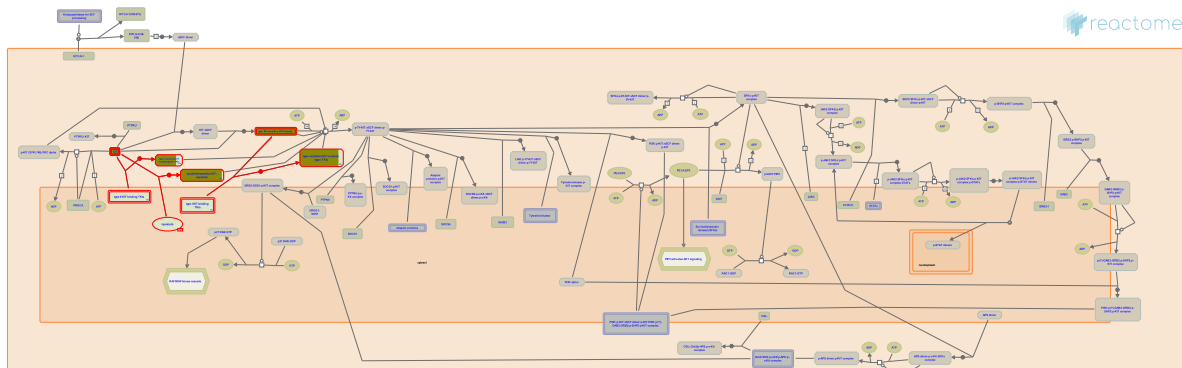
Date	Action	Author
2019-12-03	Created	Rothfels K

Date	Action	Author
2020-03-13	Reviewed	García-Valverde A, Pilco-Janeta D, Serrano C
2020-04-01	Authored	Rothfels K
2020-05-04	Edited	Rothfels K
2023-03-08	Modified	Matthews L

**1 submitted entities found in this pathway, mapping to 1 Reactome entities**

Input	UniProt Id
KIT	P10721

## 8. KIT mutants bind TKIs (R-HSA-9669921)



**Diseases:** cancer.

Aberrant signaling by activated forms of KIT can be inhibited by tyrosine kinase inhibitors. Primary mutations in KIT are frequently found in exon 11, encoding the juxtamembrane domain responsible for autoinhibition of the kinase. These mutations are generally sensitive to tyrosine kinase inhibitors such as imatinib. Accumulation of secondary mutations in the ATP-binding pocket and the activation loop of the kinase domain contributes to resistance to first line tyrosine kinase inhibitors. KIT receptors with in these regions are sensitive to a panel of additional tyrosine kinase inhibitors such as sunitinib and regorafenib (Serrano et al, 2019; reviewed in Roskoski, 2018; Klug et al, 2018; Serrano et al, 2017).

## References

- Serrano C, Mariño-Enríquez A, Tao DL, Ketzer J, Eilers G, Zhu M, ... Fletcher JA (2019). Complementary activity of tyrosine kinase inhibitors against secondary kit mutations in imatinib-resistant gastrointestinal stromal tumours. Br. J. Cancer, 120, 612-620. [🔗](#)
- Roskoski R (2018). The role of small molecule Kit protein-tyrosine kinase inhibitors in the treatment of neoplastic disorders. Pharmacol. Res., 133, 35-52. [🔗](#)
- Klug LR, Kent JD & Heinrich MC (2018). Structural and clinical consequences of activation loop mutations in class III receptor tyrosine kinases. Pharmacol. Ther., 191, 123-134. [🔗](#)
- Serrano C, George S, Valverde C, Olivares D, García-Valverde A, Suárez C, ... Carles J (2017). Novel Insights into the Treatment of Imatinib-Resistant Gastrointestinal Stromal Tumors. Target Oncol, 12, 277-288. [🔗](#)

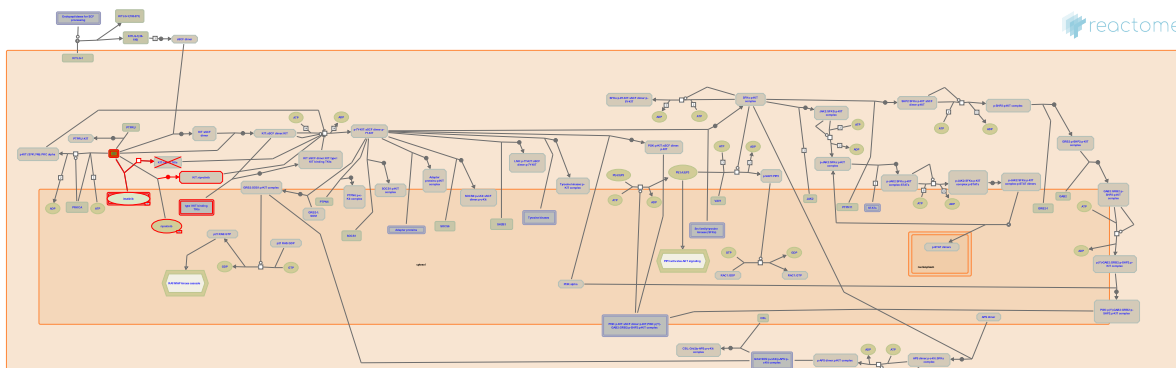
## Edit history

Date	Action	Author
2019-12-03	Created	Rothfels K
2020-03-13	Reviewed	García-Valverde A, Pilco-Janeta D, Serrano C
2020-04-01	Authored	Rothfels K
2020-05-04	Edited	Rothfels K
2023-10-12	Modified	Weiser JD

1 submitted entities found in this pathway, mapping to 1 Reactome entities

Input	UniProt Id
KIT	P10721

## 9. Imatinib-resistant KIT mutants (R-HSA-9669917)



**Diseases:** cancer.

Imatinib is approved for treatment of cancers carrying primary mutations in the KIT receptor. Imatinib binds and inhibits the inactive state of the receptor, including the conformation promoted by exon 11 mutations that relieve the auto-inhibition of the WT protein. Resistance to imatinib arises due to the polyclonal expansion of subpopulations bearing secondary KIT mutations in the ATP binding pocket or the activation loop of the protein (Serrano et al, 2019; reviewed in Roskoski, 2018; Klug et al, 2018; Corless et al, 2011).

## References

- Serrano C, Mariño-Enríquez A, Tao DL, Ketzer J, Eilers G, Zhu M, ... Fletcher JA (2019). Complementary activity of tyrosine kinase inhibitors against secondary kit mutations in imatinib-resistant gastrointestinal stromal tumours. *Br. J. Cancer*, 120, 612-620. [🔗](#)
- Roskoski R (2018). The role of small molecule Kit protein-tyrosine kinase inhibitors in the treatment of neoplastic disorders. *Pharmacol. Res.*, 133, 35-52. [🔗](#)
- Klug LR, Kent JD & Heinrich MC (2018). Structural and clinical consequences of activation loop mutations in class III receptor tyrosine kinases. *Pharmacol. Ther.*, 191, 123-134. [🔗](#)
- Corless CL, Barnett CM & Heinrich MC (2011). Gastrointestinal stromal tumours: origin and molecular oncology. *Nat. Rev. Cancer*, 11, 865-78. [🔗](#)

## Edit history

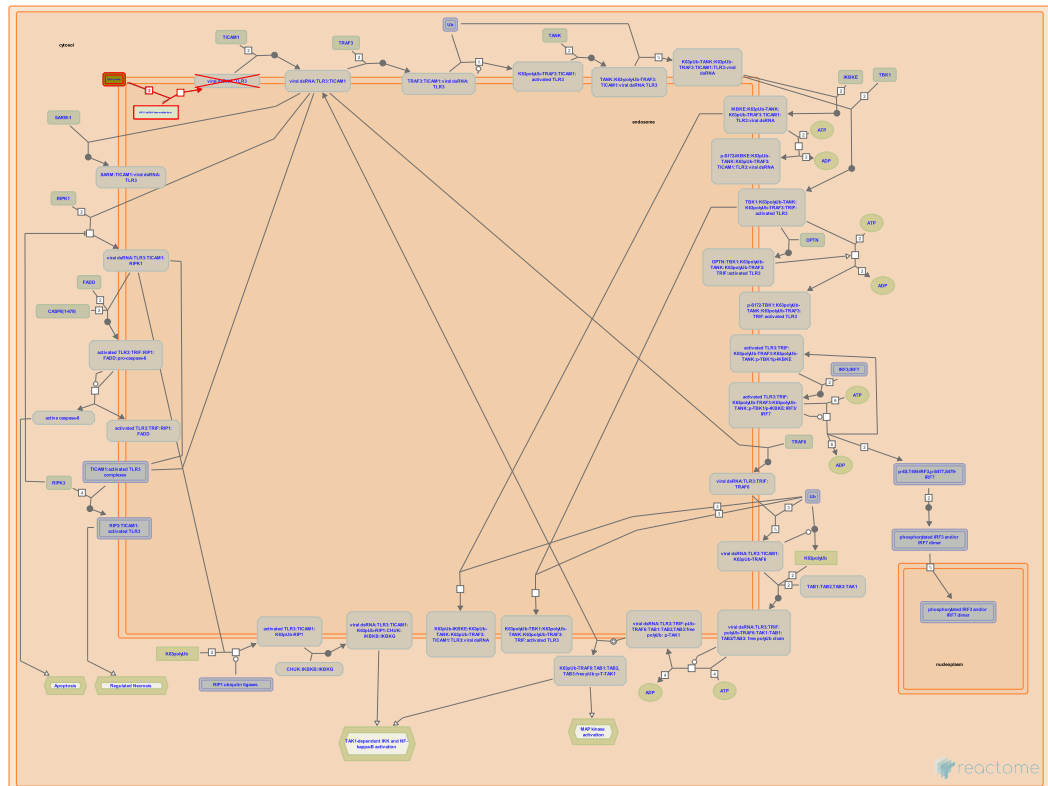
Date	Action	Author
2019-12-03	Created	Rothfels K
2020-03-13	Reviewed	García-Valverde A, Pilco-Janeta D, Serrano C
2020-04-01	Authored	Rothfels K
2020-05-04	Edited	Rothfels K
2023-03-08	Modified	Matthews L

1 submitted entities found in this pathway, mapping to 1 Reactome entities

Input	UniProt Id
KIT	P10721



## 10. TLR3 deficiency - HSE (R-HSA-5602410)



**Diseases:** primary immunodeficiency disease.

Toll like receptor 3 (TLR3) recognizes double-stranded RNA (dsRNA), an intermediate product during viral replication for most viruses. TLR3 is expressed in various tissues and cells including cells of the central nervous system (CNS) (Bsibsi M et al. 2002). TLR3 activity in neurons and glial cells was found to be critical for controlling herpes simplex virus type 1 (HSV-1) infection in CNS (Lafaille FG et al. 2012). Children with inborn errors of TLR3-mediated immunity are prone to HSV-1 encephalitis (HSE), a rare life-threatening complication during HSV-1 infection (Casrouge A et al. 2006; Perez de Diego R et al. 2010; Zhang SY et al. 2007; Herman M et al. 2012; Lafaille FG et al. 2012). The functional defect in HSE patients with TLR3 deficiency is probably due to impaired induction of type I and III interferon (IFN) by cells of the CNS, which appears to be uniquely dependent upon TLR3 for protection against HSV1 (Zhang SY et al. 2007; Guo Y et al. 2011; Lafaille FG et al. 2012). Importantly, blood cells in the periphery produce normal amounts of interferons, even in TLR3-deficient patients, which perhaps can be explained by RIGI or MDA5-mediated antiviral responses.

## References

- Guo Y, Audry M, Ciancanelli M, Alsina L, Azevedo J, Herman M, ... Zhang SY (2011). Herpes simplex virus encephalitis in a patient with complete TLR3 deficiency: TLR3 is otherwise redundant in protective immunity. *J. Exp. Med.*, 208, 2083-98. [🔗](#)
- Zhang SY, Jouanguy E, Ugolini S, Smahi A, Elain G, Romero P, ... Casanova JL (2007). TLR3 deficiency in patients with herpes simplex encephalitis. *Science*, 317, 1522-7. [🔗](#)
- Lafaille FG, Pessach IM, Zhang SY, Ciancanelli MJ, Herman M, Abhyankar A, ... Notarangelo LD (2012). Impaired intrinsic immunity to HSV-1 in human iPSC-derived TLR3-deficient CNS cells. *Nature*, 491, 769-73. [🔗](#)

Zhang SY, Abel L & Casanova JL (2013). Mendelian predisposition to herpes simplex encephalitis.  
Handb Clin Neurol, 112, 1091-7. [\[CrossRef\]](#)

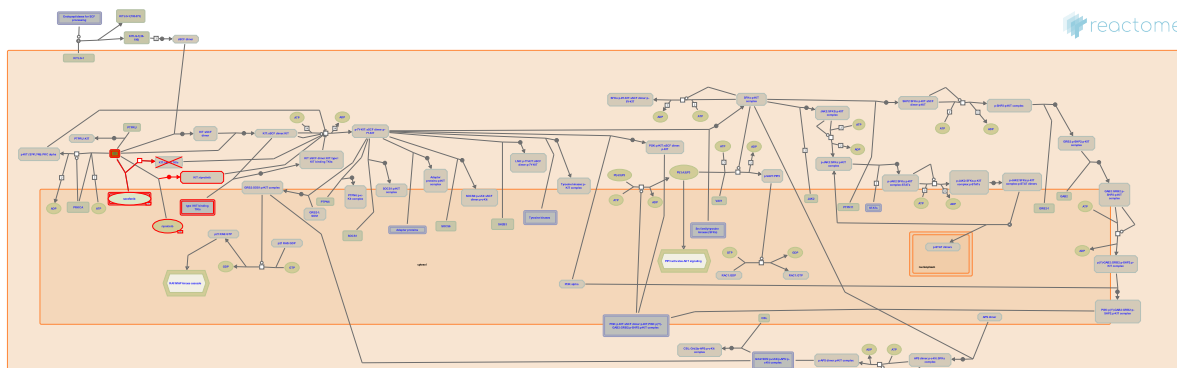
## Edit history

Date	Action	Author
2014-05-21	Authored	Shamovsky V
2014-06-24	Created	Shamovsky V
2014-09-06	Reviewed	D'Eustachio P
2015-02-10	Edited	Shamovsky V
2015-02-15	Reviewed	McDonald DR
2023-10-12	Modified	Weiser JD

**1 submitted entities found in this pathway, mapping to 1 Reactome entities**

Input	UniProt Id
TLR3	O15455

## 11. Sorafenib-resistant KIT mutants (R-HSA-9669936)



**Diseases:** cancer.

Sorafenib is a type II tyrosine kinase inhibitor that is approved for use in hepatocellular and renal cell carcinoma. It is active against KIT receptors with mutations in the ATP-binding cleft and the activation loop, with the exception of substitutions at D816, which are resistant (Guida et al, 2007; Heinrich et al, 2012; Serrano et al, 2019; Weisberg et al, 2019; reviewed in Roskoski, 2018; Klug et al, 2012).

## References

- Guida T, Anaganti S, Provitera L, Gedrich R, Sullivan E, Wilhelm SM, ... Carlomagno F (2007). Sorafenib inhibits imatinib-resistant KIT and platelet-derived growth factor receptor beta gatekeeper mutants. *Clin. Cancer Res.*, 13, 3363-9. [🔗](#)
- Heinrich MC, Mariño-Enríquez A, Presnell A, Donsky RS, Griffith DJ, McKinley A, ... Fletcher JA (2012). Sorafenib inhibits many kinase mutations associated with drug-resistant gastrointestinal stromal tumors. *Mol. Cancer Ther.*, 11, 1770-80. [🔗](#)
- Serrano C, Mariño-Enríquez A, Tao DL, Ketzer J, Eilers G, Zhu M, ... Fletcher JA (2019). Complementary activity of tyrosine kinase inhibitors against secondary kit mutations in imatinib-resistant gastrointestinal stromal tumours. *Br. J. Cancer*, 120, 612-620. [🔗](#)
- Weisberg E, Meng C, Case AE, Sattler M, Tiv HL, Gokhale PC, ... Griffin JD (2019). Comparison of effects of midostaurin, crenolanib, quizartinib, gilteritinib, sorafenib and BLU-285 on oncogenic mutants of KIT, CBL and FLT3 in haematological malignancies. *Br. J. Haematol.*, 187, 488-501. [🔗](#)
- Roskoski R (2018). The role of small molecule Kit protein-tyrosine kinase inhibitors in the treatment of neoplastic disorders. *Pharmacol. Res.*, 133, 35-52. [🔗](#)

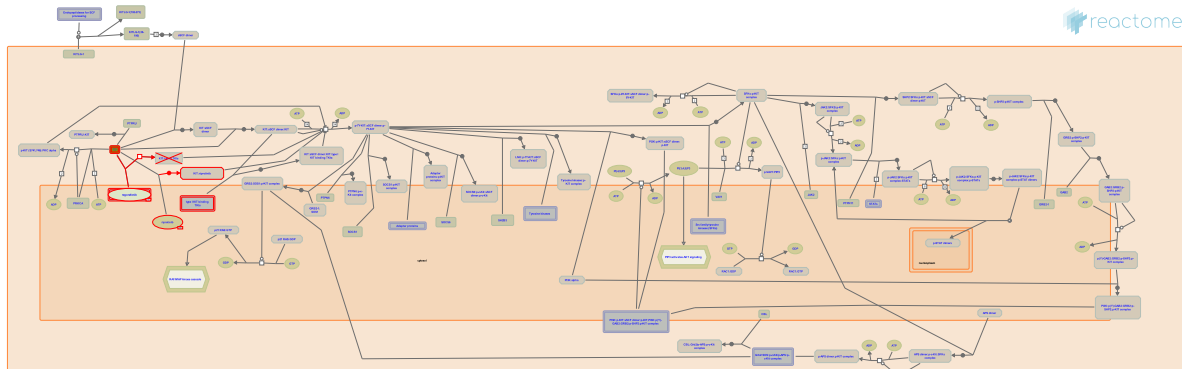
## Edit history

Date	Action	Author
2019-12-03	Created	Rothfels K
2020-03-13	Reviewed	García-Valverde A, Pilco-Janeta D, Serrano C
2020-04-01	Authored	Rothfels K
2020-05-04	Edited	Rothfels K
2023-03-08	Modified	Matthews L

1 submitted entities found in this pathway, mapping to 1 Reactome entities

Input	UniProt Id
KIT	P10721

## 12. Regorafenib-resistant KIT mutants (R-HSA-9669929)



**Diseases:** cancer.

Regorafenib is a type II tyrosine kinase inhibitor that is approved for treatment of advanced gastrointestinal stromal tumors with KIT mutations. Regorafenib is effective in imatinib-resistant tumors carrying secondary mutations in exon 14 (gatekeeper mutation), and most KIT secondary mutations encoded by exons 17 and 18 (the activation loop) (Demetri et al, 2013; Serrano et al, 2017, Serrano et al, 2019; reviewed in Roskoski, 2018; Klug et al, 2018; ).

## References

- Serrano C, Mariño-Enríquez A, Tao DL, Ketzer J, Eilers G, Zhu M, ... Fletcher JA (2019). Complementary activity of tyrosine kinase inhibitors against secondary kit mutations in imatinib-resistant gastrointestinal stromal tumours. Br. J. Cancer, 120, 612-620. [🔗](#)
- Serrano C, George S, Valverde C, Olivares D, García-Valverde A, Suárez C, ... Carles J (2017). Novel Insights into the Treatment of Imatinib-Resistant Gastrointestinal Stromal Tumors. Target Oncol, 12, 277-288. [🔗](#)
- Roskoski R (2018). The role of small molecule Kit protein-tyrosine kinase inhibitors in the treatment of neoplastic disorders. Pharmacol. Res., 133, 35-52. [🔗](#)
- Klug LR, Kent JD & Heinrich MC (2018). Structural and clinical consequences of activation loop mutations in class III receptor tyrosine kinases. Pharmacol. Ther., 191, 123-134. [🔗](#)
- Demetri GD, von Mehren M, Blanke CD, Van den Abbeele AD, Eisenberg B, Roberts PJ, ... Joensuu H (2002). Efficacy and safety of imatinib mesylate in advanced gastrointestinal stromal tumors. N. Engl. J. Med., 347, 472-80. [🔗](#)

## Edit history

Date	Action	Author
2019-12-03	Created	Rothfels K
2020-03-13	Reviewed	García-Valverde A, Pilco-Janeta D, Serrano C
2020-04-01	Authored	Rothfels K
2020-05-04	Edited	Rothfels K
2023-03-08	Modified	Matthews L

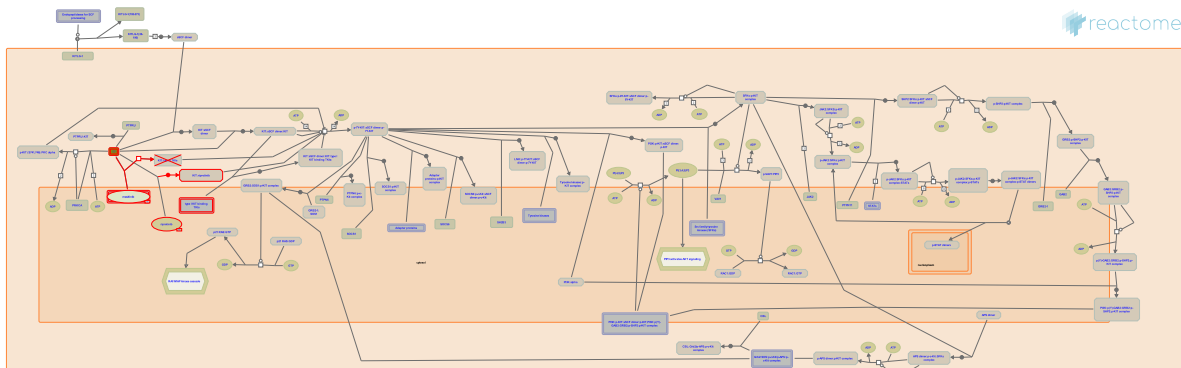
1 submitted entities found in this pathway, mapping to 1 Reactome entities

Input	UniProt Id
-------	------------

KIT

P10721

### 13. Masitinib-resistant KIT mutants (R-HSA-9669924)



**Diseases:** cancer.

Mastinib is a class II tyrosine kinase inhibitor that targets mutant and wild-type FGFR3, PDGFR and c-KIT (Dubreuil, 2009). Mastinib, like imatinib, is effective in inhibiting the activity of juxtamembrane mutant forms of KIT, but is ineffective against many of the mutations in the activation loop and ATP-binding cleft of the receptor (Dubreuil, 2009; Serrano et al, 2019; reviewed in Demetri, 2011).

### References

- Serrano C, Mariño-Enríquez A, Tao DL, Ketzer J, Eilers G, Zhu M, ... Fletcher JA (2019). Complementary activity of tyrosine kinase inhibitors against secondary kit mutations in imatinib-resistant gastrointestinal stromal tumours. *Br. J. Cancer*, 120, 612-620. [🔗](#)
- Demetri GD (2011). Differential properties of current tyrosine kinase inhibitors in gastrointestinal stromal tumors. *Semin. Oncol.*, 38, S10-9. [🔗](#)
- Dubreuil P, Letard S, Ciufolini M, Gros L, Humbert M, Castéran N, ... Hermine O (2009). Mastinib (AB1010), a potent and selective tyrosine kinase inhibitor targeting KIT. *PLoS One*, 4, e7258. [🔗](#)

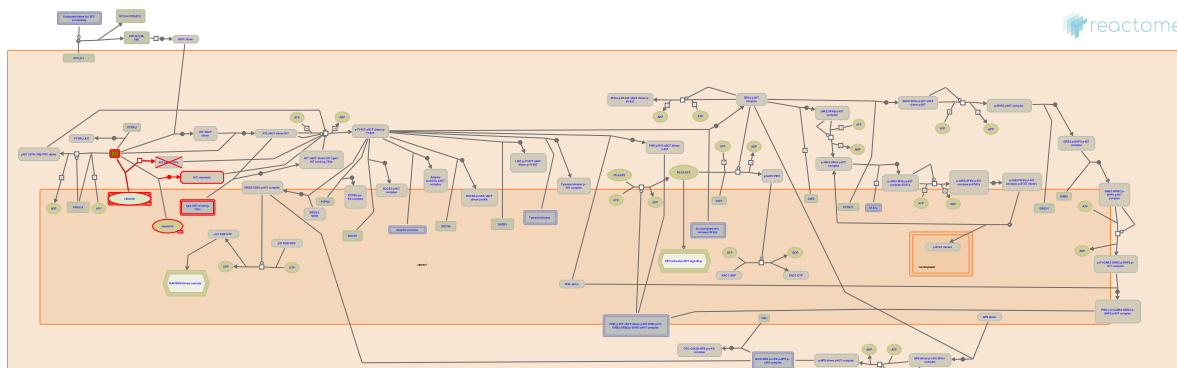
### Edit history

Date	Action	Author
2019-12-03	Created	Rothfels K
2020-03-13	Reviewed	García-Valverde A, Pilco-Janeta D, Serrano C
2020-04-01	Authored	Rothfels K
2020-05-04	Edited	Rothfels K
2023-03-08	Modified	Matthews L

1 submitted entities found in this pathway, mapping to 1 Reactome entities

Input	UniProt Id
KIT	P10721

## 14. Nilotinib-resistant KIT mutants (R-HSA-9669926)



**Diseases:** cancer.

Nilotinib is a type II tyrosine kinase inhibitor currently in clinical trials for treatment of KIT-mutant cancers, and shows variable effectiveness against mutations in exon 11, 13, 17 and 18. Nilotinib is ineffective against the gatekeeper mutation T670I (Kissova et al, 2016; Guo et al, 2007; Roberts et al, 2007; Serrano et al, 2019).

## References

- Serrano C, George S, Valverde C, Olivares D, García-Valverde A, Suárez C, ... Carles J (2017). Novel Insights into the Treatment of Imatinib-Resistant Gastrointestinal Stromal Tumors. *Target Oncol*, 12, 277-288. [\[PubMed\]](#)
- Kissova M, Maga G & Crespan E (2016). The human tyrosine kinase Kit and its gatekeeper mutant T670I, show different kinetic properties: Implications for drug design. *Bioorg. Med. Chem.*, 24, 4555-4562. [\[PubMed\]](#)
- Serrano C, Mariño-Enríquez A, Tao DL, Ketzer J, Eilers G, Zhu M, ... Fletcher JA (2019). Complementary activity of tyrosine kinase inhibitors against secondary kit mutations in imatinib-resistant gastrointestinal stromal tumours. *Br. J. Cancer*, 120, 612-620. [\[PubMed\]](#)
- Guo T, Agaram NP, Wong GC, Hom G, D'Adamo D, Maki RG, ... Antonescu CR (2007). Sorafenib inhibits the imatinib-resistant KIT(T670I) gatekeeper mutation in gastrointestinal stromal tumor. *Clin. Cancer Res.*, 13, 4874-81. [\[PubMed\]](#)
- Roberts KG, Odell AF, Byrnes EM, Baleato RM, Griffith R, Lyons AB & Ashman LK (2007). Resistance to c-KIT kinase inhibitors conferred by V654A mutation. *Mol. Cancer Ther.*, 6, 1159-66. [\[PubMed\]](#)

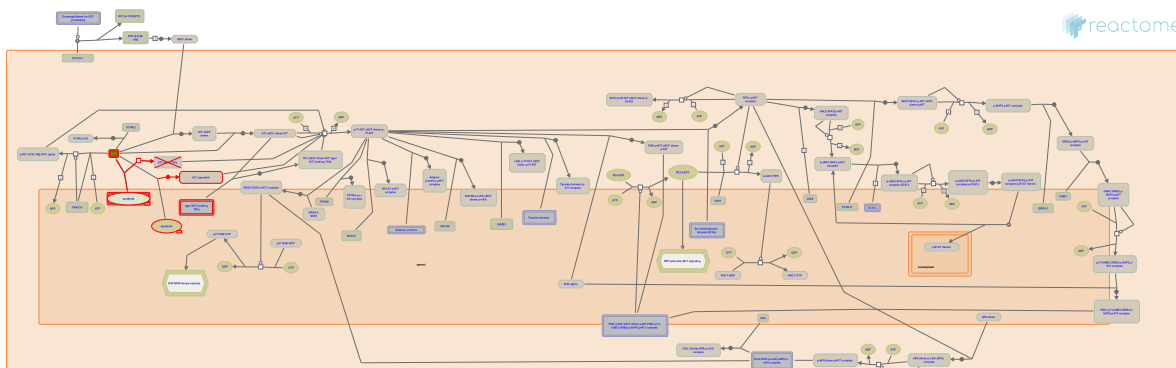
## Edit history

Date	Action	Author
2019-12-03	Created	Rothfels K
2020-03-13	Reviewed	García-Valverde A, Pilco-Janeta D, Serrano C
2020-04-01	Authored	Rothfels K
2020-05-04	Edited	Rothfels K
2023-03-08	Modified	Matthews L

**1 submitted entities found in this pathway, mapping to 1 Reactome entities**

Input	UniProt Id
KIT	P10721

## 15. Sunitinib-resistant KIT mutants (R-HSA-9669934)



**Diseases:** cancer.

Sunitinib is a class II tyrosine kinase inhibitor that is often used as a second line treatment in KIT-mutated cancers that develop resistance to imatinib (Heinrich et al, 2008; Serrano et al, 2017; reviewed in Roskoski, 2018; Corless et al, 2011).

### References

- Roskoski R (2018). The role of small molecule Kit protein-tyrosine kinase inhibitors in the treatment of neoplastic disorders. *Pharmacol. Res.*, 133, 35-52. [🔗](#)
- Serrano C, George S, Valverde C, Olivares D, García-Valverde A, Suárez C, ... Carles J (2017). Novel Insights into the Treatment of Imatinib-Resistant Gastrointestinal Stromal Tumors. *Target Oncol*, 12, 277-288. [🔗](#)
- Heinrich MC, Maki RG, Corless CL, Antonescu CR, Harlow A, Griffith D, ... Demetri GD (2008). Primary and secondary kinase genotypes correlate with the biological and clinical activity of sunitinib in imatinib-resistant gastrointestinal stromal tumor. *J. Clin. Oncol.*, 26, 5352-9. [🔗](#)

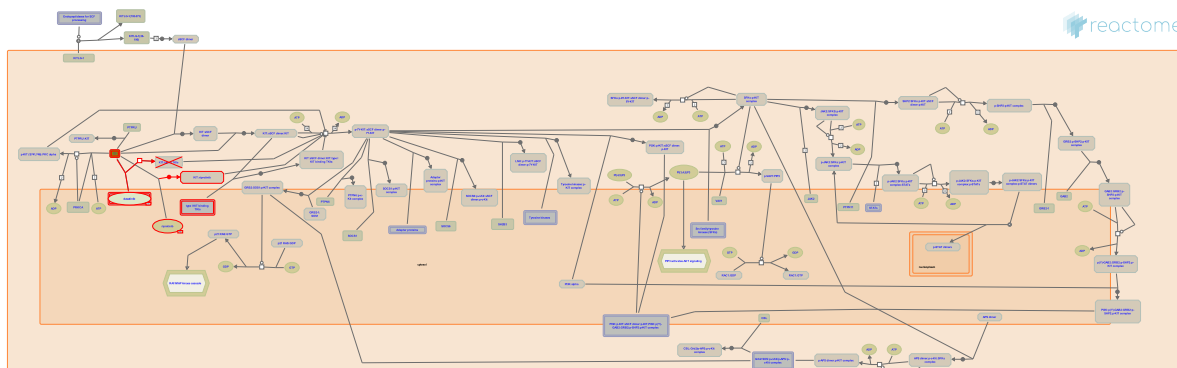
### Edit history

Date	Action	Author
2019-12-03	Created	Rothfels K
2020-03-13	Reviewed	García-Valverde A, Pilco-Janeta D, Serrano C
2020-04-01	Authored	Rothfels K
2020-05-04	Edited	Rothfels K
2023-03-08	Modified	Matthews L

1 submitted entities found in this pathway, mapping to 1 Reactome entities

Input	UniProt Id
KIT	P10721

## 16. Dasatinib-resistant KIT mutants (R-HSA-9669914)



**Diseases:** cancer.

Dasatinib is a type II tyrosine kinase inhibitor that is active against KIT receptors with mutations in the juxtamembrane and activation loop domains, but shows only partial activity against KIT receptors with mutations at residue V654 (Schittenhelm et al, 2006; Serrano et al, 2019).

### References

- Schittenhelm MM, Shiraga S, Schroeder A, Corbin AS, Griffith D, Lee FY, ... Heinrich MC (2006). Dasatinib (BMS-354825), a dual SRC/ABL kinase inhibitor, inhibits the kinase activity of wild-type, juxtamembrane, and activation loop mutant KIT isoforms associated with human malignancies. *Cancer Res.*, 66, 473-81. [\[CrossRef\]](#)
- Serrano C, Mariño-Enríquez A, Tao DL, Ketzer J, Eilers G, Zhu M, ... Fletcher JA (2019). Complementary activity of tyrosine kinase inhibitors against secondary kit mutations in imatinib-resistant gastrointestinal stromal tumours. *Br. J. Cancer*, 120, 612-620. [\[CrossRef\]](#)

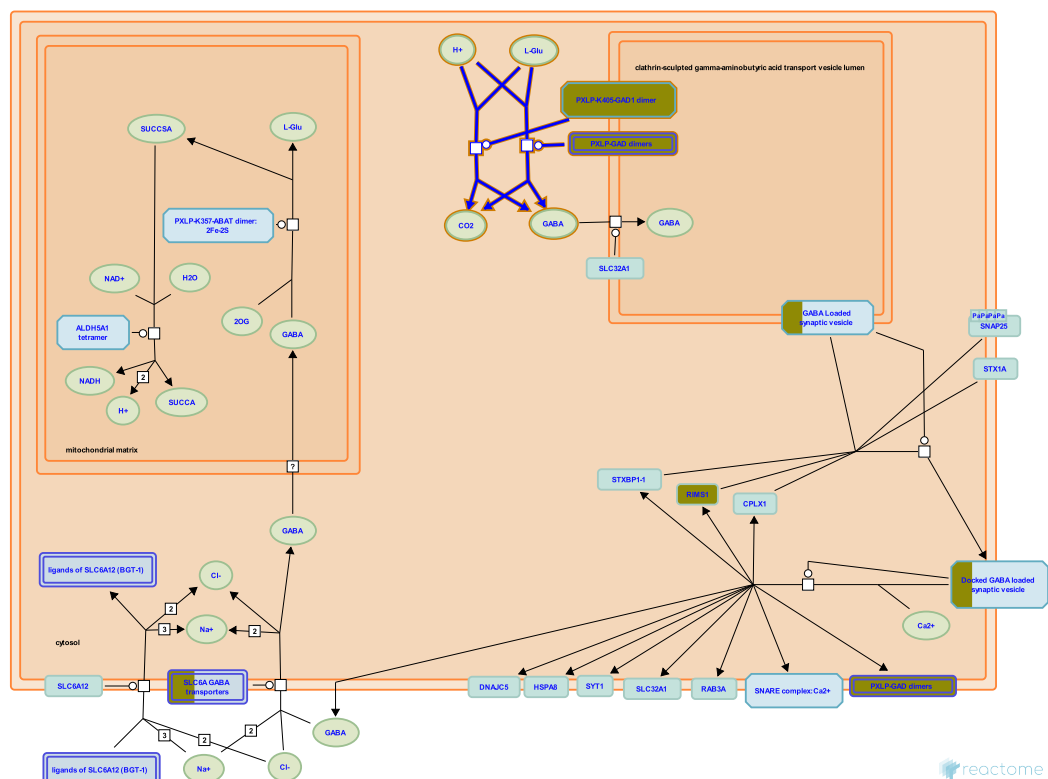
### Edit history

Date	Action	Author
2019-12-03	Created	Rothfels K
2020-03-13	Reviewed	García-Valverde A, Pilco-Janeta D, Serrano C
2020-04-01	Authored	Rothfels K
2020-05-04	Edited	Rothfels K
2023-03-08	Modified	Matthews L

1 submitted entities found in this pathway, mapping to 1 Reactome entities

Input	UniProt Id
KIT	P10721

## 17. GABA synthesis (R-HSA-888568)



**Cellular compartments:** cytosol, clathrin-sculpted gamma-aminobutyric acid transport vesicle membrane.

GABA synthesized uniquely by two forms of glutamate decarboxylases, GAD65 and GAD67, that are functionally distinct and have different co-factor requirements. GAD65 is functionally linked to VGAT, the GABA transporter and selectively GABA synthesized by GAD65 is preferably loaded into the synaptic vesicles. GABA synthesized by GAD67 may be used for functions other than neurotransmission.

## References

- Petroff OA (2002). GABA and glutamate in the human brain. *Neuroscientist*, 8, 562-73. [🔗](#)
- Soghomonian JJ & Martin DL (1998). Two isoforms of glutamate decarboxylase: why?. *Trends Pharmacol Sci*, 19, 500-5. [🔗](#)
- Martin DL & Barke KE (1998). Are GAD65 and GAD67 associated with specific pools of GABA in brain?. *Perspect Dev Neurobiol*, 5, 119-29. [🔗](#)

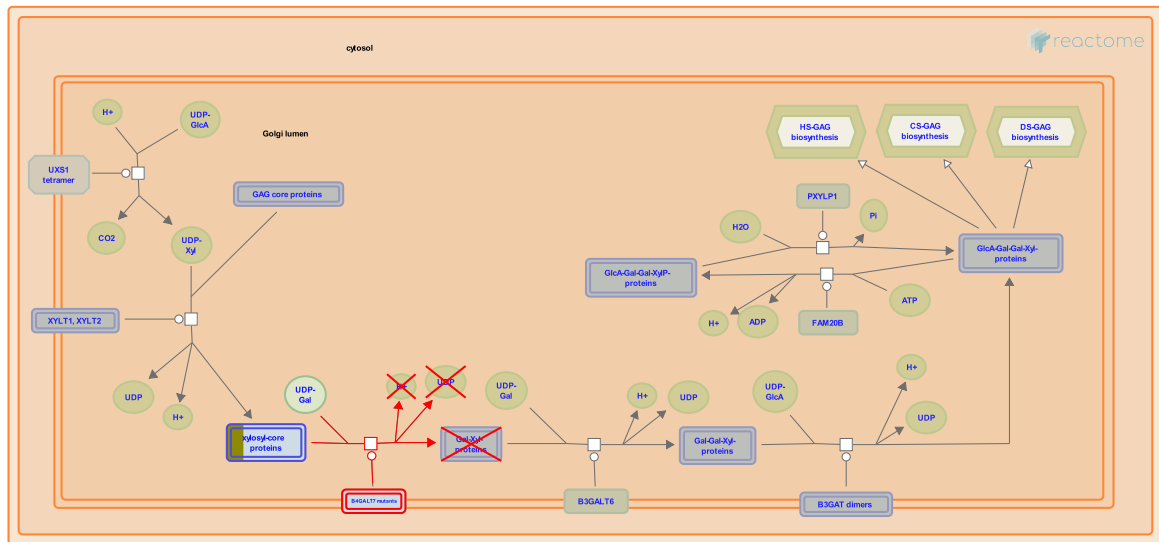
## Edit history

Date	Action	Author
2008-11-27	Reviewed	Restituito S
2010-06-30	Edited	Mahajan SS
2010-06-30	Authored	Mahajan SS
2010-06-30	Created	Mahajan SS
2025-11-15	Modified	Weiser JD

**1 submitted entities found in this pathway, mapping to 2 Reactome entities**

Input	UniProt Id
GAD1	Q05329, Q99259

## 18. Defective B4GALT7 causes EDS, progeroid type (R-HSA-3560783)



**Diseases:** Ehlers-Danlos syndrome.

Ehlers-Danlos syndrome (EDS) is a group of inherited connective tissue disorders, caused by a defect in the synthesis of collagen types I or III. Abnormal collagen renders connective tissues more elastic. The severity of the mutation can vary from mild to life-threatening. There is no cure and treatment is supportive, including close monitoring of the digestive, excretory and particularly the cardiovascular systems. Defective B4GALT7, a galactosyltransferase important in proteoglycan synthesis, causes the progeroid variant of EDS (MIM:130070). Features include an aged appearance, developmental delay, short stature, generalized osteopenia, defective wound healing, hypermobile joints, hypotonic muscles, and loose but elastic skin (Okajima et al. 1999).

### References

Okajima T, Fukumoto S, Furukawa K & Urano T (1999). Molecular basis for the progeroid variant of Ehlers-Danlos syndrome. Identification and characterization of two mutations in galactosyltransferase I gene. *J Biol Chem*, 274, 28841-4. [View](#)

### Edit history

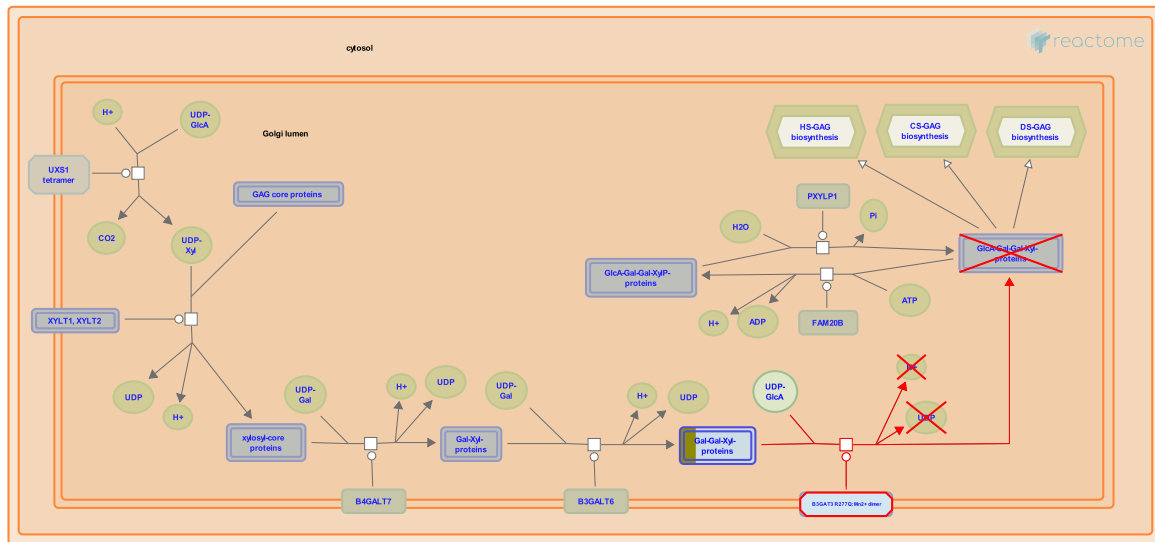
Date	Action	Author
2013-05-21	Edited	Jassal B
2013-05-21	Authored	Jassal B
2013-05-21	Created	Jassal B
2014-07-09	Reviewed	Spillmann D
2025-06-02	Modified	Stephan R

4 submitted entities found in this pathway, mapping to 4 Reactome entities

Input	UniProt ID	Input	UniProt ID
BGN	P21810	CSPG5	O95196
GPC2	Q8N158	GPC5	P78333



## 19. Defective B3GAT3 causes JDSSDHD (R-HSA-3560801)



**Diseases:** congenital heart defect, Larsen syndrome.

Galactosylgalactosylxylosylprotein 3-beta-glucuronosyltransferases1, 2 and 3 (B3GAT1-3) are involved in forming the linker tetrasaccharide present in heparan sulfate and chondroitin sulfate. Defects in B3GAT3 cause multiple joint dislocations, short stature, craniofacial dysmorphism, and congenital heart defects (JDSSDHD; MIM:245600). This is an autosomal recessive disease characterized by dysmorphic facies, elbow, hip and knee dislocations, clubfeet, short stature and cardiovascular defects (Steel & Kohl 1972, Bonaventure et al. 1992, Baasanjav et al. 2011). JDSSDHD has phenotypic similarities to Larsen syndrome (Larsen et al. 1950).

## References

- Steel HH & Kohl EJ (1972). Multiple congenital dislocations associated with other skeletal anomalies (Larsen's syndrome) in three siblings. *J Bone Joint Surg Am*, 54, 75-82. [🔗](#)
- Bonaventure J, Lasselin C, Mellier J, Cohen-Solal L & MAROTEAUX P (1992). Linkage studies of four fibrillar collagen genes in three pedigrees with Larsen-like syndrome. *J. Med. Genet.*, 29, 465-70. [🔗](#)
- Baasanjav S, Al-Gazali L, Hashiguchi T, Mizumoto S, Fischer B, Horn D, ... Hoffmann K (2011). Faulty initiation of proteoglycan synthesis causes cardiac and joint defects. *Am. J. Hum. Genet.*, 89, 15-27. [🔗](#)
- LARSEN LJ, SCHOTTSTAEDT ER & BOST FC (1950). Multiple congenital dislocations associated with characteristic facial abnormality. *J. Pediatr.*, 37, 574-81. [🔗](#)

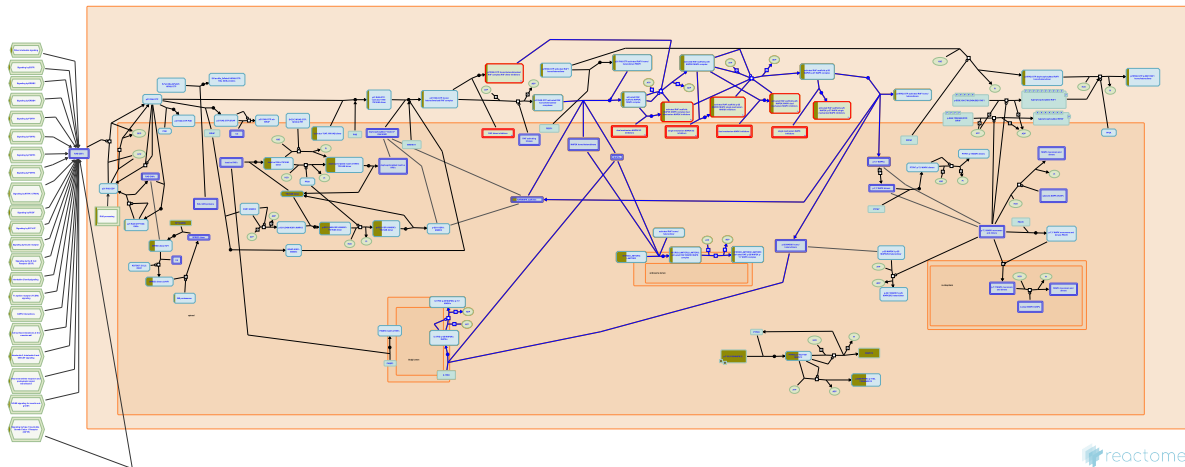
## Edit history

Date	Action	Author
2013-05-21	Edited	Jassal B
2013-05-21	Authored	Jassal B
2013-05-21	Created	Jassal B
2014-07-09	Reviewed	Spillmann D
2025-06-02	Modified	Stephan R

**4 submitted entities found in this pathway, mapping to 4 Reactome entities**

Input	UniProt Id	Input	UniProt Id
BGN	P21810	CSPG5	O95196
GPC2	Q8N158	GPC5	P78333

## 20. MAP2K and MAPK activation (R-HSA-5674135)



Activated RAF proteins are restricted substrate kinases whose primary downstream targets are the two MAP2K proteins, MAP2K1 and MAP2K2 (also known as MEK1 and MEK2) (reviewed in Roskoski, 2010, Roskoski, 2012a). Phosphorylation of the MAP2K activation loop primes them to phosphorylate the primary effector of the activated MAPK pathway, the two MAPK proteins MAPK3 and MAPK1 (also known as ERK1 and 2). Unlike their upstream counterparts, MAPK3 and MAPK1 catalyze the phosphorylation of hundreds of cytoplasmic and nuclear targets including transcription factors and regulatory molecules (reviewed in Roskoski, 2012b). Activation of MAP2K and MAPK proteins downstream of activated RAF generally occurs in the context of a higher order scaffolding complex that regulates the specificity and localization of the pathway (reviewed in Brown and Sacks, 2009; Matallanas et al, 2011).

## References

- Roskoski R Jr (2012). ERK1/2 MAP kinases: structure, function, and regulation. *Pharmacol. Res.*, 66, 105-43. [🔗](#)
- Roskoski R Jr (2012). MEK1/2 dual-specificity protein kinases: structure and regulation. *Biochem. Biophys. Res. Commun.*, 417, 5-10. [🔗](#)
- Roskoski R Jr (2010). RAF protein-serine/threonine kinases: structure and regulation. *Biochem. Biophys. Res. Commun.*, 399, 313-7. [🔗](#)
- Matallanas D, Birtwistle M, Romano D, Zebisch A, Rauch J, von Kriegsheim A & Kolch W (2011). Raf family kinases: old dogs have learned new tricks. *Genes Cancer*, 2, 232-60. [🔗](#)
- Brown MD & Sacks DB (2009). Protein scaffolds in MAP kinase signalling. *Cell. Signal.*, 21, 462-9. [🔗](#)

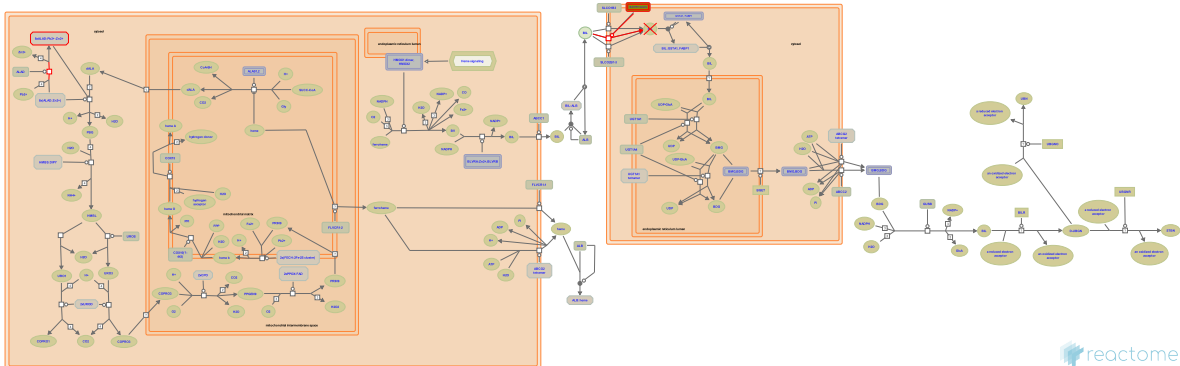
## Edit history

Date	Action	Author
2015-02-10	Authored	Rothfels K
2015-02-11	Created	Rothfels K
2015-02-12	Edited	Rothfels K
2015-04-29	Reviewed	Roskoski R Jr

6 submitted entities found in this pathway, mapping to 7 Reactome entities

Input	UniProt Id	Input	UniProt Id	Input	UniProt Id
ACTB	P60709, P63261	CSK	P41240	FGA	P02671
ITGA2B	P08514	WDR83	Q9BRX9	YWHAB	P31946

## 21. Defective SLCO1B1 causes hyperbilirubinemia, Rotor type (HBLRR) (R-HSA-5619110)



**Diseases:** bilirubin metabolic disorder.

The solute carrier organic anion transporter family member 1B1 (SLCO1B1) is expressed on the basolateral surfaces of hepatocytes and mediates the uptake of bilirubin (BIL), a breakdown product of heme degradation, to the liver where it is conjugated and excreted from the body. Defects in SLCO1B1 can cause hyperbilirubinemia, Rotor type (HBLRR; MIM:237450), an autosomal recessive form of primary conjugated hyperbilirubinemia. Mild jaundice, not associated with hemolysis, develops shortly after birth or in childhood (van de Steeg et al. 2012, Sticova & Jirsa 2013, Keppler 2014).

### References

- van de Steeg E, Stranecký V, Hartmannová H, Nosková L, Hřebíček M, Wagenaar E, ... Schinkel AH (2012). Complete OATP1B1 and OATP1B3 deficiency causes human Rotor syndrome by interrupting conjugated bilirubin reuptake into the liver. *J. Clin. Invest.*, 122, 519-28. [🔗](#)
- Sticová E & Jirsa M (2013). New insights in bilirubin metabolism and their clinical implications. *World J. Gastroenterol.*, 19, 6398-407. [🔗](#)
- Keppler D (2014). The roles of MRP2, MRP3, OATP1B1, and OATP1B3 in conjugated hyperbilirubinemia. *Drug Metab. Dispos.*, 42, 561-5. [🔗](#)

### Edit history

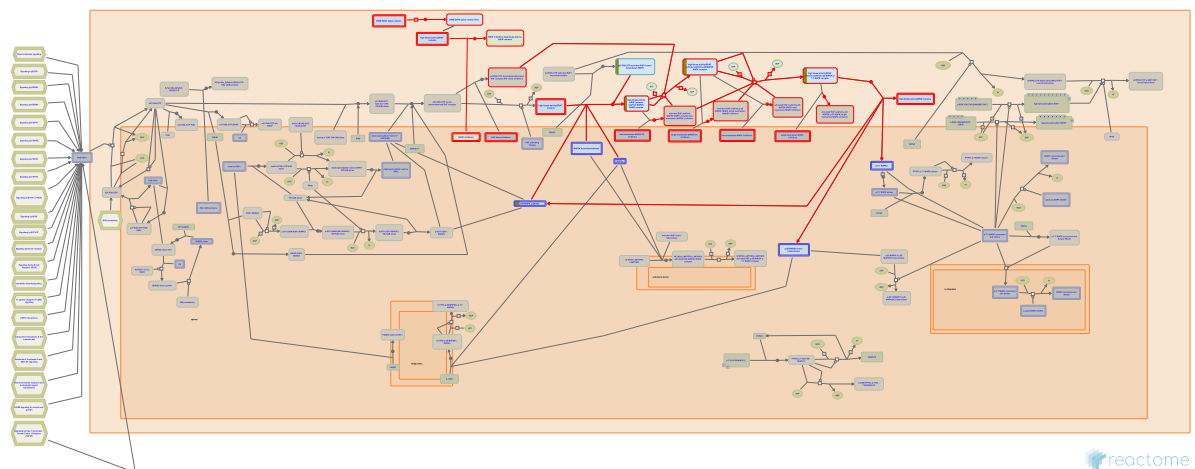
Date	Action	Author
2014-08-22	Edited	Jassal B
2014-08-22	Authored	Jassal B
2014-08-22	Created	Jassal B
2015-08-04	Reviewed	Broer S
2019-09-18	Revised	Jassal B
2023-10-12	Modified	Weiser JD

1 submitted entities found in this pathway, mapping to 1 Reactome entities

Input	UniProt Id
SLCO1B1	Q9Y6L6



## 22. Signaling by high-kinase activity BRAF mutants (R-HSA-6802948)



**Diseases:** cancer.

BRAF is mutated in about 8% of human cancers, with high prevalence in hairy cell leukemia, melanoma, papillary thyroid and ovarian carcinomas, colorectal cancer and a variety of other tumors (Davies et al, 2002; reviewed in Samatar and Poulikakos, 2014). Most BRAF mutations fall in the activation loop region of the kinase or the adjacent glycine rich region. These mutations promote increased kinase activity either by mimicking the effects of activation loop phosphorylations or by promoting the active conformation of the enzyme (Davies et al, 2002; Wan et al, 2004). Roughly 90% of BRAF mutants are represented by the single missense mutation BRAF V600E (Davies et al, 2002; Wan et al, 2004). Other highly active kinase mutants of BRAF include BRAF G469A and BRAF T599dup. G469 is in the glycine rich region of the kinase domain which plays a role in orienting ATP for catalysis, while T599 is one of the two conserved regulatory phosphorylation sites of the activation loop. Each of these mutants has highly enhanced basal kinase activities, phosphorylates MEK and ERK in vitro and in vivo and is transforming when expressed in vivo (Davies et al, 2002; Wan et al, 2004; Eisenhardt et al, 2011). Further functional characterization shows that these highly active mutants are largely resistant to disruption of the BRAF dimer interface, suggesting that they are able to act as monomers (Roring et al, 2012; Brummer et al, 2006; Freeman et al, 2013; Garnett et al, 2005). Activating BRAF mutations occur for the most part independently of RAS activating mutations, and RAS activity levels are generally low in BRAF mutant cells. Moreover, the kinase activity of these mutants is only slightly elevated by coexpression of G12V KRAS, and biological activity of the highly active BRAF mutants is independent of RAS binding (Brummer et al, 2006; Wan et al, 2004; Davies et al, 2002; Garnett et al, 2005). Although BRAF V600E is inhibited by RAF inhibitors such as vemurafenib, resistance frequently develops, in some cases mediated by the expression of a splice variant that lacks the RAS binding domain and shows elevated dimerization compared to the full length V600E mutant (Poulikakos et al, 2011; reviewed in Lito et al, 2013).

## References

- Davies H, Bignell GR, Cox C, Stephens P, Edkins S, Clegg S, ... Futreal PA (2002). Mutations of the BRAF gene in human cancer. *Nature*, 417, 949-54. [🔗](#)
- Samatar AA & Poulikakos PI (2014). Targeting RAS-ERK signalling in cancer: promises and challenges. *Nat Rev Drug Discov*, 13, 928-42. [🔗](#)

Wan PT, Garnett MJ, Roe SM, Lee S, Niculescu-Duvaz D, Good VM, ... Marais R (2004). Mechanism of activation of the RAF-ERK signaling pathway by oncogenic mutations of B-RAF. *Cell*, 116, 855-67. 

Eisenhardt AE, Olbrich H, Röring M, Janzarik W, Anh TN, Cin H, ... Brummer T (2011). Functional characterization of a BRAF insertion mutant associated with pilocytic astrocytoma. *Int. J. Cancer*, 129, 2297-303. 

Röring M, Herr R, Fiala GJ, Heilmann K, Braun S, Eisenhardt AE, ... Brummer T (2012). Distinct requirement for an intact dimer interface in wild-type, V600E and kinase-dead B-Raf signalling. *EMBO J.*, 31, 2629-47. 

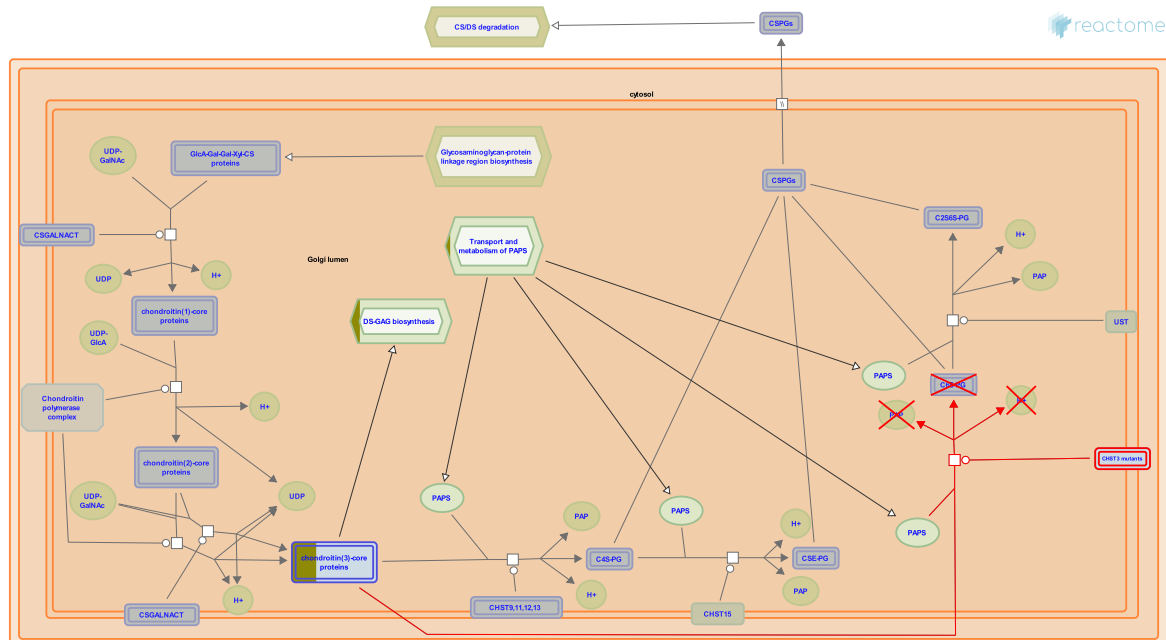
## Edit history

Date	Action	Author
2015-08-10	Edited	Rothfels K
2015-08-10	Authored	Rothfels K
2015-10-02	Created	Rothfels K
2016-08-05	Reviewed	Stephens RM

## 5 submitted entities found in this pathway, mapping to 6 Reactome entities

Input	UniProt Id	Input	UniProt Id	Input	UniProt Id
ACTB	P60709, P63261	CSK	P41240	FGA	P02671
ITGA2B	P08514	YWHAB	P31946		

## 23. Defective CHST3 causes SEDCJD (R-HSA-3595172)



**Diseases:** spondyloepimetaphyseal dysplasia.

Carbohydrate sulfotransferase 3 (CHST3) transfers sulfate ( $\text{SO}_4(2-)$ ) to position 6 of N-acetylgalactosamine (GalNAc) residues of chondroitin-containing proteins resulting in chondroitin sulfate (CS), the predominant glycosaminoglycan present in cartilage. Defects in CHST3 result in spondyloepiphyseal dysplasia with congenital joint dislocations (SEDCJD; MIM:143095), a bone dysplasia clinically characterized by severe progressive kyphoscoliosis (abnormal curvature of the spine), arthritic changes with joint dislocations and short stature in adulthood (Unger et al. 2010).

## References

Unger S, Lausch E, Rossi A, Megarbane A, Sillence D, Alcausin M, ... Superti-Furga A (2010). Phenotypic features of carbohydrate sulfotransferase 3 (CHST3) deficiency in 24 patients: congenital dislocations and vertebral changes as principal diagnostic features. Am. J. Med. Genet. A, 152, 2543-9. ↗

## Edit history

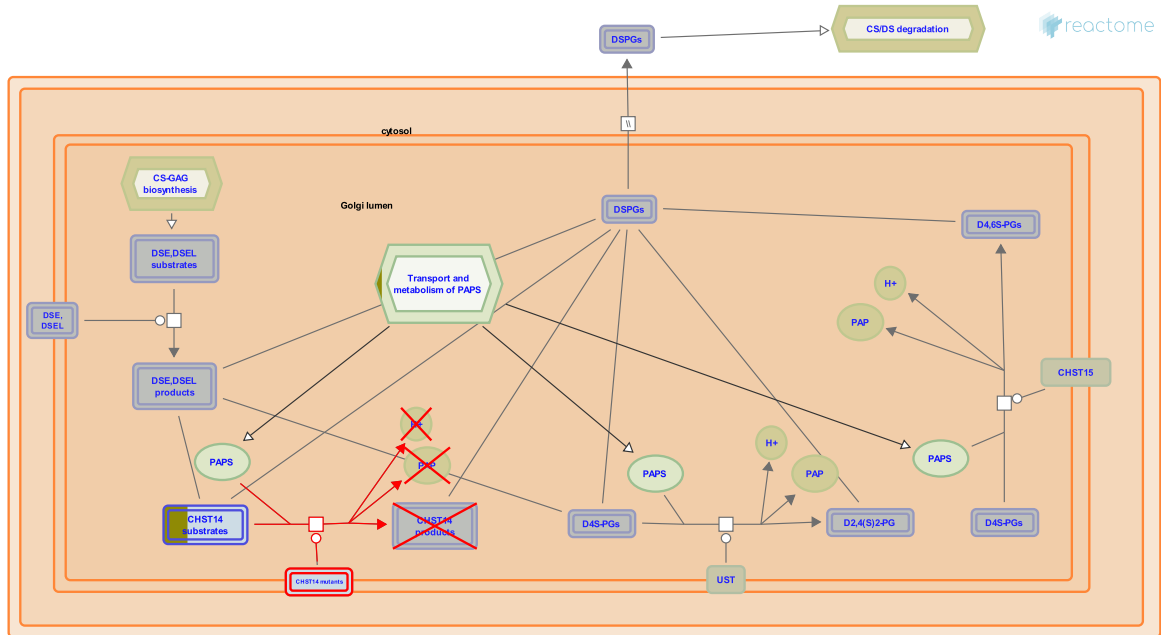
Date	Action	Author
2013-05-21	Edited	Jassal B
2013-05-21	Authored	Jassal B
2013-05-21	Created	Jassal B
2014-07-09	Reviewed	Spillmann D
2025-06-02	Modified	Stephan R

2 submitted entities found in this pathway, mapping to 2 Reactome entities

Input	UniProt Id	Input	UniProt Id
BGN	P21810	CSPG5	095196



## 24. Defective CHST14 causes EDS, musculocontractural type (R-HSA-3595174)



**Diseases:** Ehlers-Danlos syndrome.

Carbohydrate sulfotransferase 14 (CHST14 also known as D4ST-1) mediates the transfer of sulfate to position 4 of further N-acetylgalactosamine (GalNAc) residues of dermatan sulfate (DS). Defects in CHST14 cause Ehlers-Danlos syndrome, musculocontractural type (MIM:601776). The Ehlers-Danlos syndromes (EDS) are a group of connective tissue disorders that share common features such as skin hyperextensibility, articular hypermobility and tissue fragility (Beighton et al. 1998). The musculocontractural form of EDS (MIM:601776) include distinctive characteristics such as craniofacial dysmorphism, congenital contractures of fingers and thumbs, clubfeet, severe kyphoscoliosis and muscular hypotonia (Malfait et al. 2010).

## References

Beighton P, De Paepe A, Steinmann B, Tsipouras P & Wenstrup RJ (1998). Ehlers-Danlos syndromes: revised nosology, Villefranche, 1997. Ehlers-Danlos National Foundation (USA) and Ehlers-Danlos Support Group (UK). Am. J. Med. Genet., 77, 31-7. [\[link\]](#)

Malfait F, Syx D, Vlummens P, Symoens S, Nampoothiri S, Hermanns-Lê T, ... De Paepe A (2010). Musculocontractural Ehlers-Danlos Syndrome (former EDS type VIB) and adducted thumb clubfoot syndrome (ATCS) represent a single clinical entity caused by mutations in the dermatan-4-sulfotransferase 1 encoding CHST14 gene. Hum. Mutat., 31, 1233-9. [\[link\]](#)

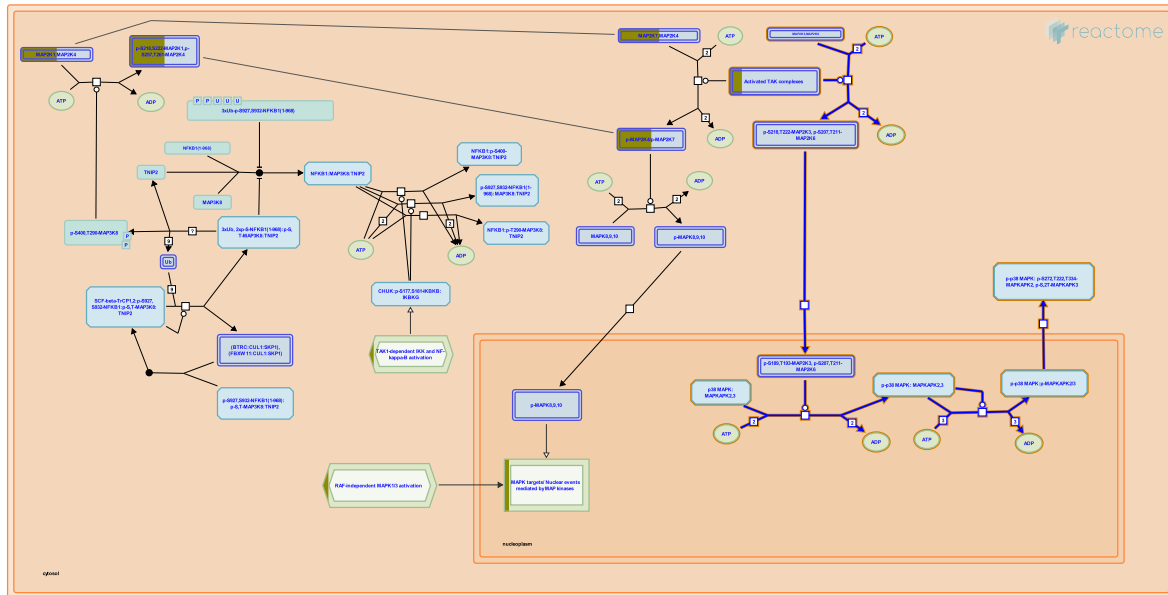
## Edit history

Date	Action	Author
2013-05-21	Edited	Jassal B
2013-05-21	Authored	Jassal B
2013-05-21	Created	Jassal B
2014-07-09	Reviewed	Spillmann D
2025-06-02	Modified	Stephan R

**2 submitted entities found in this pathway, mapping to 2 Reactome entities**

Input	UniProt Id	Input	UniProt Id
BGN	P21810	CSPG5	O95196

## 25. activated TAK1 mediates p38 MAPK activation (R-HSA-450302)



**Cellular compartments:** cytosol, nucleoplasm.

p38 mitogen-activated protein kinase (MAPK) belongs to a highly conserved family of serine/threonine protein kinases.

The p38 MAPK-dependent signaling cascade is activated by pro-inflammatory or stressful stimuli such as ultraviolet radiation, oxidative injury, heat shock, cytokines, and other pro-inflammatory stimuli. p38 MAPK exists as four isoforms (alpha, beta, gamma, and delta). Of these, p38alpha and p38beta are ubiquitously expressed while p38gamma and p38delta are differentially expressed depending on tissue type. Each isoform is activated by upstream kinases including MAP kinase kinases (MKK) 3, 4, and 6, which in turn are phosphorylated by activated TAK1 at the typical Ser-Xaa-Ala-Xaa-Thr motif in their activation loops.

Once p38 MAPK is phosphorylated it activates numerous downstream substrates, including MAPK-activated protein kinase-2 and 3 (MAPKAPK-2 or 3) and mitogen and stress-activated kinase-1/2 (MSK1/2). MAPKAPK-2/3 and MSK1/2 function to phosphorylate heat shock protein 27 (HSP27) and cAMP-response element binding protein transcription factor, respectively. Other transcription factors, including activating transcription factor 2, Elk, CHOP/GADD153, and myocyte enhancer factor 2, are known to be regulated by these kinases.

## References

Yamaguchi K, Shirakabe K, Shibuya H, Irie K, Oishi I, Ueno N, ... Matsumoto K (1995). Identification of a member of the MAPKKK family as a potential mediator of TGF-beta signal transduction . *Science*, 270, 2008-11. [🔗](#)

Thiebes A, Wolter S, Mushinski JF, Hoffmann E, Dittrich-Breiholz O, Graue N, ... Kracht M (2005). Simultaneous blockade of NFκB, JNK, and p38 MAPK by a kinase-inactive mutant of the protein kinase TAK1 sensitizes cells to apoptosis and affects a distinct spectrum of tumor necrosis factor [corrected] target genes. *J Biol Chem*, 280, 27728-41. [🔗](#)

Martin-Blanco E (2000). p38 MAPK signalling cascades: ancient roles and new functions. *Bioessays*, 22, 637-45. [🔗](#)

Li JK, Nie L, Zhao YP, Zhang YQ, Wang X, Wang SS, ... Cheng L (2016). IL-17 mediates inflammatory reactions via p38/c-Fos and JNK/c-Jun activation in an AP-1-dependent manner in human nucleus pulposus cells. *J Transl Med*, 14, 77. [🔗](#)

## Edit history

Date	Action	Author
2009-12-16	Authored	Shamovsky V
2009-12-16	Created	Shamovsky V
2010-02-28	Edited	Shamovsky V
2010-02-28	Reviewed	Gillespie ME

## 4 submitted entities found in this pathway, mapping to 4 Reactome entities

Input	UniProt Id	Input	UniProt Id
IRAK1	P51617	RIPK2	O43353
TAB1	Q15750	TAB2	Q9NYJ8

## 6. Identifiers found

Below is a list of the input identifiers that have been found or mapped to an equivalent element in Reactome, classified by resource.

**574 of the submitted entities were found, mapping to 735 Reactome entities**

Input	UniProt Id	Input	UniProt Id	Input	UniProt Id
ABCA13	Q86UQ4	ABCA2	O95477	ABCC3	O15438
ACE2	Q9BYF1	ACOT1	Q86TX2	ACOT9	Q9Y305
ACSM5	Q6NUN0	ACTB	P60709, P63261	ACTR3	P61158
ADAM20	O43506	ADAM23	O75077	ADAM8	P78325
ADAM9	Q99965	ADAMTS4	O75173	ADCY7	P51828
AGAP2	Q99490	AGK	Q53H12	ALPK1	Q96QP1
AMELX	Q99217	AMPD3	Q01432	AMY2B	P19961
ANGPTL8	Q6UXH0	ANKH	Q9HCJ1	ANPEP	P15144
AP2A1	O95782	APBB1	O00213	APOBEC4	Q8WW27
APOBR	Q0VD83	AQP5	P55064	ARF4	P18085
ARHGAP9	Q9BRR9	ARHGEF3	Q9NR81	ARL3	P36405
ARSB	P15848	ASB11	Q8WXH4	ASPSCR1	Q9BZE9
ATF6B	Q99941	ATG9B	Q674R7	ATP10D	Q9P241
ATP11B	Q9Y2G3	ATP1B2	P14415	ATP2B3	Q16720
ATP6AP2	O75787	ATP6V0A2	Q9Y487	ATP7B	P35670
AXIN2	Q9Y2T1	B3GALT6	Q96L58	B3GNT4	Q9C0J1
B3GNT5	Q9BYG0	B4GALT2	O60909	BATF	Q16520
BEST1	O76090	BGN	P21810	BHLHA15	Q7RTS1
BMI1	P35226	BMP2K	Q2M2I8	BMS1	Q14692
BOC	Q9BWV1	BSN	Q9UPA5	BTN2A1	Q7KYR7
BUD31	P41223	C19orf84	I3L1E1	C4B	P0C0L4
C6	P13671	CABLES1	Q8TDN4	CACNA1I	Q9P0X4
CACNG4	Q9UBN1	CACNG8	Q8WXS5	CAMKMT	Q7Z624
CASK	P68400	CASP5	P51878	CAST	O15446
CBLL1	Q75N03	CBR1	P16152	CBX1	P83916
CBX8	Q9HC52	CCAR1	Q8IX12	CCDC59	Q9P031
CCK	P06307	CCL25	O15444	CCR2	P51681
CD38	P28907	CDH24	Q86UP0	CDKN1C	P49918
CEP70	Q8NHQ1	CFH	P05160	CGB3	P0DN86
CHI3L1	P36222	CHRDL1	Q9BU40	CHST7	Q9NS84
CIT	O14578, O14578-3	CLDN18	P56856	CLDN8	P56748
CMAS	Q8NFW8	CNTNAP1	P78357	COL19A1	Q14993, Q9BXS0
COL20A1	Q9P218	COL6A3	A8TX70, P12111	COPG1	Q9Y678
COPG2	Q9UBF2	COX6B1	P14854	COX7A2	P14406
CPA2	P48052	CRK	P46108	CSAD	Q9Y600
CSF1	P09603	CSK	P41240	CSPG5	O95196
CST6	P04080	CTBP1	Q13363	CTNNBIP1	Q9NSA3
CTPS2	Q9NRF8	CTRC	Q99895	CXCL12	P48061
CYB5A	P00167-1	CYB5B	P00167	CYP27A1	Q02318
CYP2F1	P24903	CYSTM1	Q9H1C7	CYTH4	Q9UIA0
DAB2	P98082	DAPP1	Q9UN19	DCTN3	O75935

Input	UniProt Id	Input	UniProt Id	Input	UniProt Id
DCUN1D5	Q9BTE7	DCX	O43602	DDX23	Q9BUQ8
DDX41	Q7L591	DENND4B	O75064	DERL1	Q9GZP9
DGKG	P49619	DHH	O43323	DHX36	Q9H2U1
DIMT1	Q9UNQ2	DLL1	O00548	DMP1	Q13316
DMRT1	Q9Y5R6	DNMT3B	Q9UBC3	DOCK11	Q5JSL3
DOK1	Q93070	DOK6	Q6PKX4	DOT1L	Q8TEK3
DUOXA1	Q1HG43	DYNC1H1	Q14204	DYNC1LI1	O43237, Q9Y6G9
DYNC2LI1	Q8TCX1	DYNLRB1	Q9NP97	EARS2	Q5JPH6
ECI2	O75521-2	EDN2	P20800	EEF1AKMT1	Q8WVE0
EEF1G	P26641	EFNB1	P98172	EIF3B	P55884
ENO2	P09104	ENTPD1	P49961	ENTPD4	Q9Y227
EPHA4	P54764	EPN2	O95208	EPS8	Q12929
ERCC2	P18074	ERCC5	P28715	ERLEC1	Q96DZ1
ETF1	P62495	ETFBKMT	Q8IXQ9	ETFDH	Q16134
ETNK2	Q9NVF9	ETV4	P43268	EYS	Q13753
EZH1	Q92800	FAM169A	Q9Y6X4	FAN1	Q9Y2M0
FANCD2	Q9BXW9	FAR2	Q96K12	FGA	P02671
FGD5	Q6ZNL6	FGF14	Q92915	FHOD3	Q8IVF7
FLT3LG	P49771	FRMPD3	Q5JV73	FRS3	O43559
FTL	P02792	FUT1	P19526	FUT7	Q11130
GABRA5	P31644	GAD1	Q05329, Q99259	GADD45GIP1	Q8TAE8
GALNT11	Q8NCW6	GBA1	P04062	GBA3	Q9H227
GBE1	Q04446	GBF1	Q92538	GCNT7	Q6ZNI0
GFM1	Q96RP9	GGT5	P36269	GHRL	Q9UBU3-1, Q9UBU3-2
GIT2	Q14161	GJB7	Q6PEY0	GJC1	P36383
GLRA3	O75311	GNAT1	P11488	GNB3	P16520
GNG8	O14610, Q9UK08	GNRH2	O43555	GOLGA5	Q8TBA6
GOLGA7	Q7Z5G4	GOLGB1	Q14789	GP5	P40197
GPC2	Q8N158	GPC5	P78333	GPR162	Q8IVL6
GPR35	Q9HC97	GPX3	O75715, P22352	GRIA4	P48058
GRPEL1	Q9HAV7	GYG2	O15488	H2AZ1	P0C0S5
H4C11	P62805	H4C12	P62805	H4C6	P62805
HARS2	P49590	HBEGF	Q99075	HBQ1	P69905
HCN3	Q9P1Z3	HIP1R	O75146	HLA-DMA	P28067
HOXA4	Q00056	HSD17B4	P51659	HSPA14	Q0VDF9
HSPA1L	P34931	HSPA9	P38646	IGFBP2	P18065
IGFBP4	P22692	IGFBP5	P24593	IGHG3	P01860
IL12RB2	Q99665	IL20RA	Q9UHF4	IL21	Q9HBE4
IL3RA	P26951	INPP5D	Q92835	INTS14	Q96SY0
IPO5	O00410	IRAK1	P51617	IRF3	Q92985
IRF5	Q13568	ITGA2B	P08514	ITGAD	P20702
ITGB4	P16144	JAG2	Q9Y219	JCHAIN	P01591
JOSD2	Q8TAC2	KANK1	Q14678	KCN2	Q9Y6J6
KCNH7	Q9NS40	KCNJ4	P48050	KCNK4	Q9NYG8
KDM3B	Q7LBC6	KDM4C	Q9H3R0	KDM4D	Q6B0I6
KDM5D	Q9BY66	KHDRBS3	O75525	KHK	P50053
KIF26B	Q2KJY2	KIRREL1	Q96J84	KIT	P10721
KLHL13	Q9P2J3, Q9P2N7	KPNA1	P52294	KRBA1	A5PL33
KRT20	P35900	KRT34	P02533	KRT78	Q8N1N4

Input	UniProt Id	Input	UniProt Id	Input	UniProt Id
KRTAP5-2	Q6L8H2, Q701N4	KYAT3	Q6YP21	LAS1L	Q9Y4W2
LEO1	Q8WVC0	LIPG	Q9Y5X9	LMAN1	P49257
LOXL3	P58215	LPCAT1	Q8NF37	LRG1	P02750
LRRTM2	O43300	LTF	P02788	MAGOHB	P61326, Q96A72
MAN2C1	Q9NTJ4	MAP2K5	Q13163	MAP3K5	Q99683
MAPK12	P53778	MCCC1	Q96RQ3	MCEMP1	Q8IX19
MECOM	Q03112	MED17	Q9NVC6	MFN1	Q8IWA4
MGAT5B	Q3V5L5	MIS18BP1	Q6P0N0	MITF	O75030-9
MIXL1	Q9H2W2	MKNK1	Q9BUB5	MKRN1	Q9UHC7
MKRN3	P31947	MLANA	Q16655	MMP10	P08254, P09238
MMP15	P51511	MOV10L1	Q9BXT6	MRPL22	Q9NWU5
MRRF	Q96E11	MRS2	Q9HD23	MRTFA	Q969V6
MSRB3	Q8IXL7	MT2A	P02795	MT3	P25713
MTERF3	Q96E29	MTMR14	Q8NCE2	MTOR	P42345
MTRES1	Q9P0P8	MTRF1	O75570	MUC13	Q9H3R2
MUC5AC	P98088	MUC6	Q6W4X9	MUL1	O15151
MYBPC3	Q14896	MYO15A	Q9UKN7	NAAA	Q02083
NANS	Q9NR45	NAPG	Q99747	NCSTN	Q92542
NEK11	Q8NG66	NEK4	P45985	NEO1	O43861
NEURL1	O76050	NF1	P21359	NFATC1	O95644
NFE2L2	Q16236	NHLRC2	Q8NBF2	NLRC4	Q9NPP4
NMT1	P30419	NOSTRIN	Q8IVI9	NPC1L1	Q9UHC9-2
NPPC	P23582	NR1D1	P20393	NR1I3	Q14994-1, Q14994-2
NSDHL	Q15738	NT5C1B	Q96P26, Q9BXI3	NUDT15	Q9NV35
NUDT3	O95989	NUP188	Q5SRE5	OCRL	Q01968
ONECUT1	Q9UBC0	OPHN1	O60890	OPRD1	P41143
OPRK1	P41145	OR13C5	Q8NGS8	OR1J1	Q8NGS3
OR1J2	Q8NGS2	OR1J4	Q8NGS1	OR4F29	Q6IEY1
OR51B4	Q9Y5P0	OR52E8	Q6IFG1	OR52N2	Q8NGI0
OTUD7A	Q8TE49	PADI3	Q9ULW8	PAK4	O96013
PCGF2	P35227	PDE8A	O60658	PDGFC	Q9NRA1-1
PDK2	Q15119	PDILIM5	Q96HC4	PDP2	Q9P2J9
PDS5A	Q29RF7	PDX1	P52945	PEX14	O75381
PGM3	O95394	PIGG	Q5H8A4	PILRB	Q9UKJ0
PLA2G6	O60733	PLA2G7	Q13093	PLAU	P00749
PLD4	Q96BZ4	PLEKHG4	Q58EX7	PLIN3	Q8IUC6
PLN	P26678	PLXNA3	P51805	PLXNB1	O43157
PLXNB3	O43157	PNPLA7	Q6ZV29	POLH	Q9Y253
POLR1B	Q9H9Y6	POLR3H	Q9Y535	POM121	Q96HA1
PPFIA1	Q13136	PPIL2	Q13356	PPM1B	O75688
PPP1R12B	O60237	PPP1R8	Q12972	PPT2	Q9UMR5
PRICKLE1	Q96MT3	PRPF4	O43172	PRPF8	Q6P2Q9
PSCA	O43653	PSMA4	P25789	PSMD2	Q13200
PTH2R	P49190	PTS	Q03393	PWP2	Q15269
PYGL	P06737	RAB33A	Q14088	RAB44	Q7Z6P3
RAB9A	P51151	RABEP1	Q15276	RABGGTA	Q92696
RABGGTB	P53611	RAC3	P60763	RALB	P11234
RBL1	P28749	RBM8A	Q9Y5S9	RFC2	P35249, P35250
RHBG	Q9H310	RHOT1	Q8IXI2	RIMS1	Q86UR5

Input	UniProt Id	Input	UniProt Id	Input	UniProt Id
RIPK2	O43353	RND3	P61587	RNF123	Q5XPI4
RNF34	Q969K3	RNPC3	Q96LT9	ROPN1	Q9HAT0
RPL28	P46776, P46779	RPL36AL	Q969Q0	RPP38	P78345
RPS27	P42677, Q71UM5	RRAGA	Q5VZM2, Q7L523	RRM1	P23921
RSAD2	Q8WXG1	RUNX2	Q13950-1, Q13950-2	RYR1	P21817
SAE1	Q9UBE0	SAT1	Q9H2B4	SCN11A	Q9UI33
SDHD	O14521	SEC11A	P67812	SEC22B	O75396
SEC24B	O95487	SEC61A1	P61619	SECISBP2	Q96T21
SERP1	Q9Y6X1	SERPINB11	P30740	SERPINB8	P50452
SFTPD	P35247	SH3GL3	P82987	SHB	Q15464
SHC2	P98077	SIKE1	Q9BRV8	SIRPB1	O00241
SLAMF7	Q9NQ25	SLC22A13	Q9Y226	SLC24A4	Q8NFF2
SLC39A3	Q9BRY0	SLC40A1	Q9NP59	SLC44A5	Q8NCS7
SLC45A2	Q9UMX9	SLC47A1	Q96FL8	SLC4A2	P04920
SLC4A5	Q9BY07	SLC5A4	Q9NY91	SLC6A13	Q9NSD5
SLC9C1	Q4G0N8	SLC9C2	Q5TAH2	SLCO1A2	P46721
SLCO1B1	Q9Y6L6	SMAP2	Q9H0E9	SMN1	Q16637
SMS	P52788	SNIP1	Q8TAD8	SNW1	Q13573
SORD	Q00796	SOX2	P48431	SPINK5	Q9NQ38
SPSB3	Q6PJ21	SRP54	P61011	SSB	P05455
STRADB	Q9C0K7	STX1B	P61266	SULT1A2	P50226
SUMF1	Q8NBK3	SVIP	Q8NHG7	SYN2	Q9NY99
TAB1	Q15750	TAB2	Q9NYJ8	TAF5L	O75529
TAP1	Q03518	TAS2R10	Q9NYW0	TAS2R50	P59544
TBC1D10B	Q4KMP7	TBC1D14	Q9P2M4	TBC1D4	O60343
TBL3	Q12788	TBX1	O43435	TCN2	P20062
TDG	Q13569	TECTA	O75443	TEX12	Q9BXU0
THEM5	Q8N1Q8	TIGAR	Q9NQ88	TIMP1	P01033
TLR1	Q15399, Q9Y2C9	TLR3	O15455	TMEM132A	Q24JP5
TMEM59	Q9BXS4	TMPO	P42167	TNFRSF14	Q92956
TNFRSF25	Q93038	TOP1	P11387	TP53AIP1	Q9HCN2
TPM1	P09493	TPTE2	P56180, Q6XPS3	TRAPPC8	Q9Y2L5
TRIM14	Q14142	TRIM2	Q9C040	TRIM48	Q8IWZ4
TRIM71	Q2Q1W2	TRIM9	Q9C026	TTLL3	A6PVC2, Q9Y4R7
TTYH3	Q9C0H2	TUT1	Q9H6E5	TXK	P42681
UBE2D2	P62837	UBE2F	Q969M7	UBE2V2	Q15819
UBL5	Q9BZL1	UBXN7	O94888	UGT1A8	Q9HAW9
UQCRRH	P07919	USP16	Q9Y5T5	USP2	O75604
USP21	Q9UK80	USP44	Q70CQ1, Q9H0E7	USP47	Q96K76
VPREB3	Q9UKI3	VPS18	Q9P253	VPS37A	Q8NEZ2
VRK2	Q86Y07	WBP4	O75554	WDR77	Q9BQA1
WDR82	Q6UXN9	WDR83	Q9BRX9	WDTC1	Q8N5D0
WFDC2	P19957	WNK1	Q9H4A3	WNT11	O96014
WNT5B	Q9H1J7	XCL1	P47992, Q9UBD3	XPC	Q01831
XRCC4	Q13426	YWHAB	P31946	ZBTB17	Q13105
ZDHHC9	Q9Y397	ZNF154	A6NNF4, Q13106	ZNF208	O43345
ZNF23	P17027	ZNF250	P15622	ZNF398	Q9BS31
ZNF425	Q6IV72	ZNF479	Q96JC4	ZNF484	Q5JVG2, Q8N8J6
ZNF556	Q9HAH1	ZNF573	Q86YE8	ZNF621	Q6ZSS3

Input	UniProt Id	Input	UniProt Id	Input	UniProt Id
ZNF627	Q7L945	ZNF638	Q14966	ZNF665	Q9H7R5
ZNF701	Q9NV72	ZNF764	Q96H86	ZNF767P	Q75MW2

Input	Ensembl Id	Input	Ensembl Id	Input	Ensembl Id
ABCC3	ENSG00000108846	ACTB	ENST00000331789	AMY2B	ENST00000361355
ANPEP	ENST00000300060	ATP6AP2	ENSG00000182220	AXIN2	ENSG00000168646, ENST00000307078
BATF	ENSG00000156127	BHLHA15	ENST00000609256	BOC	ENSG00000144857
CCR2	ENSG00000121807	CGB3	ENSG00000104827	CPA2	ENST00000222481
CSF1	ENSG00000184371	CTRC	ENST00000375949	CXCL12	ENSG00000107562
DHH	ENSG00000139549	DLL1	ENSG00000198719	DMRT1	ENSG00000137090
EPHA4	ENSG00000116106	FAN1	ENSG00000075618	FANCD2	ENSG00000144554, ENST00000419585
FTL	ENST00000331825	GAD1	ENSG00000128683	GHRL	ENSG00000157017
HOXA4	ENSG00000197576, ENST00000360046	HSPA1L	ENSG00000206383, ENSG00000226704, ENSG00000234258, ENSG00000236251	HSPA9	ENSG00000113013
IL12RB2	ENSG00000081985	IRAK1	ENSG00000184216	IRF3	ENSG00000126456
IRF5	ENSG00000128604	ITGA2B	ENSG00000005961	KDM4C	ENST00000381306
KIT	ENST00000288135	MECOM	ENSG00000085276	MIR34A	ENSG00000207865
MITF	ENSG00000187098	MIXL1	ENST00000366810	MLANA	ENSG00000120215
MMP10	ENSG00000166670	MT2A	ENSG00000125148	NFE2L2	ENSG00000116044
NLRC4	ENSG00000091106	NR1D1	ENSG00000126368	ONECUT1	ENST00000305901
OPRD1	ENSG00000116329	OPRK1	ENSG00000082556	OR13C5	ENSG00000277556
OR1J1	ENSG00000136834	OR1J2	ENSG00000197233	OR1J4	ENSG00000239590
OR4F29	ENSG00000230178, ENSG00000284662, ENSG00000284733	OR51B4	ENSG00000183251	OR52E8	ENSG00000183269
OR52N2	ENSG00000180988	PDX1	ENST00000381033	RABGGTA	ENSG00000100949
RBL1	ENSG00000080839	RSAD2	ENSG00000134321	RUNX2	ENSG00000124813
SERP1	ENSG00000120742	SFTP2	ENSG00000133661	SOX2	ENSG00000181449
TIGAR	ENSG00000078237	TIMP1	ENSG00000102265	TP53AIP1	ENSG00000120471
TRIM14	ENSG00000106785	TRIM2	ENSG00000109654	TRIM48	ENSG00000150244
UCA1	ENST00000645805	WFDC2	ENSG00000101443	WNT11	ENSG00000085741
ZBTB17	ENSG00000116809				

Input	ChEBI Id
CIT	16947

Input	miRBase Id	Input	miRBase Id	Input	miRBase Id
MIR34A	MI0000268	MIR429	MI0001641	MIRLET7B	MI0000063

## Interactors (654)

Input	UniProt Id	Interacts with	Input	UniProt Id	Interacts with
AATK	Q6ZMQ8	P36873	ACE2	Q9BYF1	Q13685
ACOT1	Q86TX2	P05549	ACOT9	Q9Y305	P13671
ACTB	EBI-5276484	P26358	ACTR3	P61157	O00401
ADAM23	Q9UKQ2	P00749	ADAM8	P78325	P42680
ADAM9	Q13443	Q99962	ADAMTS4	O75173	O00462
ADCK5	Q3MIX3	Q7Z3S9	AGAP2	Q8CGU4	Q8IZJ1

Input	UniProt Id	Interacts with	Input	UniProt Id	Interacts with
AGK	Q53H12	Q9Y5J6	AKAP7	Q9P0M2	P17612
AMPD3	Q01432	P08238	ANGPTL7	O43827	P17987
ANGPTL8	Q6UXH0	Q96PM5	ANKRA2	Q9H9E1	P56524
ANKRD36	A1A5B0	Q08379	ANKRD52	Q8NB46	P53350
ANXA8	P13928	Q00403	AP2A1	O95782	P29353
APBB1	O00213	Q07954	API5	Q9BZZ5-2	P19404
APOBEC4	Q8WW27	P55212	AQP5	P55064	P61978
ARF4	P18085	Q96PM5	ARHGAP9	Q9BRR9	P62993
ARHGEF3	Q9NR81	P14373	ARL3	Q9WUL7, P36405	A6NIH7, O75695
ARSB	P15848	P01185	ASAP2	O43150	P19174
ASPSCR1	Q9BZE9	P55072	ASTN1	O14525-2	Q14145
ATF6B	Q99941	Q8TC07	ATG9B	Q674R7	Q9Y496
ATP11B	A0A0C4DG94	A6NI15	ATP6AP2	O75787	Q15904
ATP6V0A2	Q9Y487	P01730	ATP7B	P35670	O00244
AXIN2	Q9Y2T1	Q99728	B3GALT6	Q96L58	P40855
BACE2	Q9Y5Z0	P10997	BATF	Q16520	P18848
BCAS4	Q8TDM0	Q96EV8	BCL2L12	Q9HB09	Q07812
BEND5	Q7L4P6	Q8N8N7	BEX1	Q9HBH7	Q9NRD5
BEX2	Q9BXY8	P19883	BHLHA15	Q7RTS1	Q9H4P4
BMI1	P35226	P17096	BMP2K	Q9NSY1	Q8WY64
BMS1	Q14692	P62753	BOC	Q9BWV1	Q14623
BRSK2	Q8IWQ3-3	Q9Y4K3	BTBD18	B2RXH4	Q9UBU9
BTN2A1	Q7KYR7-4	Q8IY26	BUD31	P41223	Q9NRD5
C15orf48	Q9C002	P42858	C16orf87	Q6PH81	Q9UM11
C17orf97	Q6ZQX7-4	P08684	C1orf220	Q5T0J3	Q9NV35
C1orf226	A1L170	P53350	C4orf33	Q8N1A6	P55212
C6	P13671	Q6Y288	CABLES1	Q8TDN4	P80370
CALR3	Q96L12	Q8WXG9	CAMKMT	Q7Z624	P02452
CAPRIN2	Q6IMN6	O75197	CASK	O14936	Q13009
CASP5	P51878	P49662	CAST	O15446	O15160, O95602, P19388, P61218
CAVIN4	Q5BKX8	Q13895	CBLC	Q9ULV8	Q9BQP7
CBLL1	Q9JIY2	P12830	CBR1	P16152	O75828
CBX1	P83916	P62805	CBX8	Q9HC52	P11686
CCAR1	Q8IX12	P52294	CCDC103	Q8IW40	P26367
CCDC184	Q52MB2	Q13114	CCDC185	Q8N715	Q86TI0
CCDC59	Q9P031	P98164	CCDC88B	A6NC98	P20700
CCK	P06307	Q8WUX9	CCL25	O15444	P13501, P48061
CCN3	P48745	O43559	CCNI	Q14094	Q00535
CCNI2	Q6ZMN8	Q00535	CDCA7	Q9BWT1	O76024
CDCA7L	Q96GN5	Q6NZI2	CDKN1C	P49918	P11802
CENPV	Q7Z7K6	Q92993	CEP112	Q8N8E3	P31947
CEP70	Q8NHQ1	Q99728	CERCAM	Q5T4B2	Q9Y5V3
CFAP100	Q494V2-2	P07237	CFAP298	P57076	O00628
CFAP47	Q6ZTR5	P0CG47	CFH	P08603	P01024
CGB3	P0DN86	P01215	CHI3L1	P36222	P17931
CHRNB1	P11230	Q5T9L3	CHST7	Q9NS84	P40855
CIT	O14578	O14907	CKAP2	Q8WWK9	Q13257
CLCC1	Q96S66	P59632	CLDN18	P56856	Q08426
CLDN8	P56748	Q3SXY8	CLHC1	Q8NHS4	Q96ES7

Input	UniProt Id	Interacts with	Input	UniProt Id	Interacts with
CMAS	Q8NFW8	P48059	CMYA5	Q8N3K9	O75923
CNNM2	Q9H8M5	Q12974	CNPY4	Q8N129	Q9BRQ8
CNTNAP1	P78357	Q9H2A9	COL6A3	P12111	Q6ISS4
COPG1	Q9Y678	Q9NTJ5	COPG2	Q9UBF2	P27824, P04233
COX6B1	P14854	P00403	COX7A2	P14406	P00403
CPA2	P48052	P11021	CRACDL	Q6NV74	P47756
CRK	P46108	P16234	CSAD	Q9Y600	Q9NRF2-2
CSF1	P09603	Q7Z3S9	CSK	P41240	Q68CZ2
CSPG5	O95196	P54198	CST6	Q15828	P07711
CT55	Q8WUE5	Q9Y316	CTBP1	Q13363	O43474
CTNNBIP1	Q9NSA3	Q9BRT9	CTPS2	Q9NRF8	Q8IWZ8
CTRC	Q99895	Q8NBK3	CXCL12	P48061	P78556, P13501, O15444, Q99616
CXorf58	Q96LI9	Q9NZC3	CYB5A	P00167	P51572
CYB5B	O43169	Q8WWI5	CYSTM1	Q9H1C7	Q6ZMH5
CYTH4	Q9UIA0	P20618	DAB2	P98078, P98082	Q9UM54
DAPP1	Q9UN19	Q8WY64	DCLK1	O15075	O43602
DCLK2	Q8N568	P62258	DCTN3	O75935	Q9Y244
DCUN1D5	Q9BTE7	Q9NRD5	DCX	O43602	Q9BSE5
DDX23	Q9BUQ8	P62316, P62306, P14678, P62304	DDX27	Q96GQ7	Q15646
DDX41	Q9UJV9	P14678	DDX54	Q8TDD1	Q15646
DDX56	Q9NY93	P62753	DERL1	Q9BUN8	Q05329
DHH	O43323	Q4KMG0	DHX36	Q9H2U1	Q16629
DIMT1	Q9UNQ2	P19320	DMRT1	Q9Y5R6	Q9Y5R6
DMWD	G5E9A7	Q8WW38	DMXL2	Q8TDJ6	O75695
DNMT3B	Q9UBC3	P48552	DNTTIP2	Q5QJE6	Q6NZI2
DOCK11	Q5JSL3	P31946	DOK1	Q99704	P46109
DOK6	Q6PKX4	Q16288	DOT1L	Q8TEK3	P35222
DRICH1	Q6PGQ1	P49674	DUSP12	Q9UNI6	P55010
DYNC1H1	Q14204	P43034	DYNC1LI1	Q9Y6G9	P43034
DYNC2LI1	Q8TCX1	Q14203	DYNLRB1	Q9NP97	P10636-8
E4F1	Q66K89	P67809	EARS2	Q5JPH6	Q9Y639
ECEL1	O95672	Q13217	ECI2	O75521	P13569
EEF1AKMT1	Q8WVE0	P68104	EEF1G	P26641, P26641-2	P68104, P29692, P24534
EFNB1	P98172	O15397	EGFL8	Q99944	P08311
EIF2D	P41214	P17980	EIF3B	P55884	Q04637, P06730
ELAVL3	Q14576	Q13627	ENO2	P09104	P06733
ENTPD1	P49961	Q96S59	EPHA4	P54764	P05177
EPN2	O95208-2	Q86T03	EPS8	Q12929	P49419
ERCC2	P18074	P15056	ERCC5	P28715	P15056
ERLEC1	Q96DZ1	Q9H2A9	ETF1	P62495	P04798
ETFBKMT	Q8IXQ9	P10809	ETNK2	Q9NVF9	Q16623
ETV4	P43268-3	Q13485	ETV5	P41161	Q8NHY2
EWSR1	Q01844	Q13114	EZH1	Q92800	P15056
FAM114A1	Q8IWE2	Q9UBN6	FAM124A	Q86V42	Q96QF0
FAM169A	Q9Y6X4	P20700	FAM170A	A1A519	Q93009
FAM210B	Q96KR6	P09601	FAM3B	P58499	O75197
FAM83H	Q6ZRV2	P49674	FAN1	Q16658	P54278
FANCD2	Q9BXW9	O00255	FAR2	Q96K12	P40855

Input	UniProt Id	Interacts with	Input	UniProt Id	Interacts with
FEZ1	Q9Y250	P30307	FGA	P02671	P02647
FGD5	Q6ZNL6	P55212	FGF14	Q92915-2	P49638
FHOD3	Q2V2M9, Q2V2M9-4	Q13501	FIZ1	Q96SL8	Q04721
FKBP15	Q5T1M5	O95816	FMC1	Q96HJ9	Q9NUJ1
FMR1NB	Q8N0W7	Q9HCG8	FNDC3A	Q9Y2H6	O43511
FOXR1	Q6PIV2	O95619	FRS3	O43559	Q96FE5
FTL	P02792	Q8WVC6	FUT1	P19526	Q92521
FYCO1	Q9BQS8	Q9GZQ8	GAD1	Q99259	Q13188
GADD45GIP1	Q8TAE8	P40763	GALNT11	Q8NCW6	Q15116
GBA1	P04062	P51159	GBF1	Q92538	O43914
GFM1	Q96RP9	P03508	GGT5	P36269	Q03426
GIT2	Q14161	Q13177	GJB7	Q6PEY0	Q9NWQ8
GJC1	P36383	P43119	GLCCI1	Q86VQ1	Q13627
GMEB1	Q9Y692	Q13114	GMEB2	Q9UKD1	Q13114
GNG8	Q9UK08	P49959	GNL2	Q13823	P62753
GOLGA5	Q8TBA6	Q8NCH0	GOLGA7	Q7Z5G4	P0DTC2
GOLGB1	Q14789	Q9Y3A6	GPATCH2L	Q9NWQ4-1	Q96RU7
GPC5	P78333	Q13485	GPR155	Q7Z3F1	P25090
GPR182	O15218	Q9BVG9	GPR35	Q9HC97	P17931
GRIA4	P48058-2	Q8WTS1	GRPEL1	Q9HAV7	P07902
H2AZ1	P0C0S5	P62805	H4C11	P62805	P0DTC4
H4C12	P62805	P0DTC4	H4C6	P62805	P0DTC4
HARS2	P49590	P12081	HBEGF	Q99075	P00533
HBQ1	P09105	P02100, P02042, P68871, P69892	HIC2	Q96JB3	Q96KQ7
HIP1R	O75146	Q9NZQ7	HIVEP1	P15822	P84022
HLA-DMA	P28067	P02686	HMGB3	O15347	Q02548
HOXC9	P31274	Q06710	HSD17B4	P51659	P13569
HSPA14	Q0VDF9	Q8IWL3	HSPA1L	P34931	Q13233
HSPA9	P38646	Q9H1K1	HUNK	P57058	P23528, P53667
IER5	Q5VY09	Q00613	IFFO1	Q0D2I5, Q0D2I5-5	Q13426
IGBP1	P78318	Q92993	IGFBP2	P18065	P59665
IGFBP4	P22692	P05019	IGFBP5	P24593	Q9UBD6
IGFBPL1	Q8WX77	P43146	IGHG3	P01860	P30838
IKZF3	Q9UKT9	P11802	IL12RB2	Q99665	Q14765
IL20RA	Q9UHF4	Q99741	IL3RA	P26951-1	P08700
INKA1	Q96EL1	Q9HAQ2	INPP5D	Q92835, Q92835-2	Q75525
INTS14	Q96SY0	P67775	IPO5	O00410	Q05513
IRAK1	P51617	Q92985	IRF3	Q14653	Q96EN8
IRF5	Q13568	Q13568	IRX6	P78412	Q96RU7
ITGA2B	P08514-1	P21333	ITGB4	P16144	P48509, Q15149
ITPRIPL2	Q3MIP1	Q9BRI3	JCHAIN	P01591	O94844
JOSD2	Q8TAC2	P49638	KANK1	Q14678	Q9UQB8
KCNJ4	P48050	Q9HAP6	KCTD17	Q8N5Z5	P11686
KDM3B	Q7LBC6	P09917	KDM5D	Q9BY66-3	P10275
KHDRBS3	O75525	Q8WX92	KHK	P50053-2	P50458
KIFBP	Q96EK5	Q15185	KIRREL1	Q96J84	Q07157
KIT	P10721	Q14451	KLHL13	Q9P2N7	P01282
KLHL6	Q8WZ60	Q13485	KPNA1	P52294	P20700

Input	UniProt Id	Interacts with	Input	UniProt Id	Interacts with
KRBA1	A5PL33	P14373	KRT20	P35900	Q7Z3S9
KRT34	O76011	Q9NQ94	KRTAP5-2	Q701N4	P07438
LAS1L	Q9Y4W2	O00410	LEO1	Q8WVC0	O00267
LIMCH1	Q9UPQ0-1	Q96JA1	LIPG	Q9Y5X9	Q9Y3A6
LMAN1	P49257	P04578	LPCAT1	Q8NF37	O14975
LRCH2	Q5VUJ6	Q13309	LRFN5	Q96NI6	P23468, Q13332
LRG1	P02750	P99999	LRRC46	Q96FV0	Q9UM11
LRRC59	Q96AG4	P04049	LRRC73	Q5JTD7	Q6UWV6
LRRTM2	O43300	P01375	LTF	P02788	Q9HA64
MACROH2A1	O75367	P17096	MAGEA4	P43358	Q5SW96
MAGEC1	O60732	O43463	MAGEC3	Q8TD91-2	P78333
MAGEL2	Q9UJ55	Q9UMX1	MAGOHB	Q96A72	Q13573
MAP1A	P78559	Q9GZQ8	MAP2K5	Q13163	Q13164
MAP3K21	Q5TCX8	O15111	MAP3K5	Q99683	P25445
MAP3K9	P80192	P17252	MAP7D3	Q8IWC1	P61981
MAPK12	P53778	Q14160	MARCHF3	Q86UD3	Q12959
MARK1	Q9P0L2	P0DTD2	MCCC1	Q96RQ3	P47985
MCEMP1	Q8IX19	Q6ZPD8	MECOM	Q03112	P01100
MED17	Q9NVC6	Q15648	MEIS3	Q99687-3	O14964
METTL17	Q9H7H0	Q9UBX5	MFN1	Q8IWA4	Q16611
MFSD3	Q96ES6	Q8N4V1	MFSD9	Q8NBP5	P35414
MICALL2	Q8IY33	P12814	MIDN	Q504T8	P22736
MIS18BP1	Q6P0N0	P56539	MISP	Q8IVT2	P17707
MITD1	Q8WV92	P04618	MITF	O75030	P19484
MKI67	P46013	P53667	MKNK1	Q9BUB5	Q16539
MKRN1	Q9UHC7	P51668	MKRN2	Q9H000	P51668
MKRN3	Q13064	Q13882	MLANA	Q16655	P51810
MMP10	P09238	P01033	MOB3B	Q86TA1	Q13188
MORC3	Q14149	Q9NWF9	MROH1	Q8NDA8	Q9Y639
MRPL22	Q9NWU5	P62241	MRRF	Q96E11	P11182
MRS2	Q9HD23	Q9H244	MRTFA	Q969V6	P11831
MSRB3	Q8IXL7	Q9UKN5	MT2A	P02795	P09429
MTERF3	Q96E29	P22732	MTOR	P42345	Q9NZQ7
MUL1	Q969V5	P63279	MXD1	Q05195	Q96ST3
MYORG	Q6NSJ0	P80370	NAPG	Q99747	O15155
NCKAP5L	Q9HCH0	Q9NV70	NCSTN	Q92542	P35613
NECAB1	Q8N987	O00244	NEK11	Q8NG66	P51955
NEK4	P51957	P12235	NF1	P21359	P21709
NFATC1	O95644	P18846	NFATC4	Q14934	P0CG48
NFE2L2	Q16236	O60675	NHLRC2	Q8NBF2-2	P04792
NKD1	Q969G9	P67775	NLRC4	Q9NPP4	P29466, Q9NPP4
NMT1	P30419	P04601	NOSTRIN	Q8IVI9	Q05193
NPM3	O75607	P40429	NR1D1	P20393	P06727
NR1I3	Q14994	P01100	NRIP2	Q9BQI9	Q8N9N5
NUCB2	P80303	P24522	NUCD3	Q8IVD9	P43034
NUP188	Q5SRE5	P19320	NUP62CL	Q9H1M0	O14641
NYAP2	Q9P242	P52594	OCRL	Q01968	Q9NYZ3
OIT3	Q8WWZ8	P49639	OPRD1	P41143	Q9UKG4
OPRK1	P41145	P35414	OSGIN1	Q9UJX0	Q9Y6K9
OTUD7A	Q8TE49	Q13485	OTULINL	Q9NUU6	Q8NBQ5

Input	UniProt Id	Interacts with	Input	UniProt Id	Interacts with
OTX1	P32242	Q9Y6K1	PADI3	Q9ULW8	P27361
PAGE1	O75459	P22732	PAK4	O96013	O00401
PAQR7	Q86WK9	P40763	PAX9	P55771	O43474
PCBD2	Q9H0N5	P35680	PCDHA3	Q9Y5H8	Q16850
PCGF2	P35227	Q93009	PDCL3	Q9H2J4	Q13371
PDGFC	Q9NRA1	P16234	PDK2	Q15119	Q16654
PDLIM5	Q96HC4	P11142	PDS5A	Q29RF7	Q7Z5K2
PDX1	O00330	Q8IWL3	PDZD2	O15018	P59637
PEX14	O75381	P40855	PGBD1	Q96JS3	P22736
PHYHIP	Q92561	Q9NS87	PIGG	Q5H8A4	Q13304
PIH1D1	Q9NWS0	Q7KZ85, Q96JC9	PIH1D2	Q8WWB5	O60469
PIK3IP1	Q96FE7	P78382	PLA2G6	O60733	O60733
PLAU	P00749	Q03405	PLEKHG4	Q58EX7	Q9NQ94
PLIN3	O60664	Q05329	PLN	P26678	Q8N661
PLXNB1	O43157	Q92730	PLXNB3	Q9ULL4	P08581
POC1B	Q8TC44	Q9BRX2	POGLUT3	Q7Z4H8	P0DTC8
POLH	Q9Y253	Q86YC2	POLR1B	Q9H9Y6	O15160, O95602, P19388, P61218, Q3B726, P62875
POLR3H	Q9Y535	P61081	POM121	Q96HA1-2	Q13114
PPFIA1	Q13136	O95995	PPM1B	O75688	P05161
PPP1R12B	O60237-2	Q14957	PPP1R8	Q12972, Q12972-2	P36873
PPTC7	Q8NI37	P11182	PRICKLE1	Q96MT3	Q9HAQ2
PROSER3	Q2NL68	Q96ES7	PRPF4	O43172	P62316, P62306, P14678
PRPF8	Q6P2Q9	Q9UJV9	PSMA4	P25789	Q16665
PSMD2	Q13200	Q9Y4K3	PTH2R	P49190	P13591
PTPRM	P28827	O60469	PTS	Q03393	Q96CW1
PWP1	Q13610	P48431	PWP2	Q15269	Q8IWZ6
PYGL	P06737	Q13451	QRICH1	Q2TAL8	Q14938
RAB33A	Q14088	Q8IUQ4	RAB9A	P51151	Q92696, P53611
RABEP1	Q15276	Q9NZ52	RABGGTA	Q92696	P53611
RABGGTB	P53611	Q9UBV7	RAC3	P60763	P52565
RALB	P11234	P52306	RANBP3L	Q86VV4	Q08379
RASSF3	Q86WH2	Q9UER7	RBL1	P28749	O43524
RBM8A	Q9Y5S9	Q92900	RCN3	Q96D15	Q9UMX1
RCSD1	Q6JBY9	P52907	RFC2	P35250	P40937, P35249
RFX2	P48378	O75928-2	RGPD5	Q99666	P61769
RHOT1	Q8IXI2	O60260	RIMS1	Q86UR5	P06241
RIPK2	O43353	Q13114	RND3	P61587	O43157
RNF123	Q5XPI4	Q9BQ52	RNF34	Q969K3	Q14790
RNPC3	Q96LT9	P62306, P14678, P62304	ROPN1	Q9HAT0	P24588
RP9	Q8TA86	P67870	RPL28	P46779	P43146
RPL36AL	Q969Q0	P03372	RPP38	P78345	P06748
RPS27	P42677	Q00987	RRAGA	Q7L523	P61916
RRM1	P23921	P31350	RRP12	Q5JTH9	Q00839
RSAD2	Q8WXG1	P55056, P02654	RTL8B	Q17RB0	O00560
RUNX2	Q13950	P17480	RUSF1	Q96GQ5	Q6ZPD8
RYR1	P11716	P62942	S100A13	Q99584	P01375
SAE1	Q9UBE0	Q06710	SAMD11	Q96NU1	Q96RU7
SAR1A	Q9NR31	P78382	SASH1	O94885	P31947
SAT1	Q9H2H9	Q9UKG4	SCAF8	Q9UPN6	Q08379

Input	UniProt Id	Interacts with	Input	UniProt Id	Interacts with
SCML1	Q9UN30-2	O00560	SCRN1	Q12765	Q15750
SEC11A	P67812	P06276	SEC22B	O75396	O95249, Q13190
SEC24B	O95487	Q15436	SEC61A1	P61619	Q16288
SECISBP2	Q96T21	Q08379	SERF1B	O75920	A1L3X0
SERP1	Q9Y6X1	Q12846	SERPINB8	P50452	Q15696
SESTD1	Q86VW0	Q15561	SFTPД	P35247, P35247-PRO_0000017465	P0DTC2
SH2D3A	Q9BRG2	P00533	SH3GL3	Q99963	Q99962
SH3YL1	Q96HL8	Q5HYK7	SHB	Q15464	P00519
SHROOM1	Q2M3G4	P31946	SIKE1	Q9BRV8	O43815
SIRPB1	O00241	O43914	SLAMF7	Q8BHK6	P06241
SLC25A41	Q8N5S1	P98082	SLC25A48	Q6ZT89	Q13077
SLC39A3	Q9BRY0	P32971	SLC40A1	Q9JHI9	O60674
SLC44A5	Q8NCS7	P50454	SLC6A13	Q9NSD5-3	P04792
SLCO1B1	Q9Y6L6	Q9NPD5	SMAP2	Q9H0E9	O96019
SMN1	Q16637	Q96FZ7	SNIP1	Q8TAD8	P59595
SNW1	Q13573	P46531	SORBS2	O94875	Q13177
SOX2	P48431	P30740	SPEF1	Q9Y4P9	O96006
SPRYD4	Q8WW59	P24534	SPSB3	Q6PJ21	Q93034, Q9UBF6
SRP54	P61011	P11142	SSB	P05455	Q8WZA2
STPG2	Q8N412	P02787	STRADB	Q9C0K7	Q15831
STRIP1	Q5VSL9	Q9BRV8	STX1B	P61266	O15554
STXBP6	Q8NFX7	Q13277	SUMF1	Q8NBK3	Q8NBK3, Q8NBJ7
SURF6	O75683	P78563	TAB1	Q15750	Q9Y4K3
TAB2	Q9NYJ8	Q9Y4K3	TAF5L	O75529	O43524
TAL2	Q16559	Q99081	TAP1	Q03518	P07237
TBC1D14	Q9P2M4	O75385	TBC1D4	O60343	P31947
TBL3	Q12788	P06748	TCEAL1	Q15170	Q16539
TCN2	P20062	Q9NPF0	TDG	Q13569	Q15788
TEKT5	Q96M29	Q9NPB3	TENM2	Q9NT68	P21926
TENT5B	Q96A09	O95947	TEX12	Q9BXU0	Q13153
TGFB1I1	O43294	Q14289	TIGAR	Q9NQ88	P41247
TIMP1	P01033	P14780, P09238	TLR1	Q15399	O60603
TLR3	O15455	O15455	TM2D2	Q9BX73	P29033
TM2D3	Q9BRN9	P0DTC8	TM4SF19	Q96DZ7	P09601
TMCC2	O75069	Q96T88	TMED6	Q8WW62	Q16585
TMEM132A	Q24JP5	Q01523	TMEM154	Q6P9G4	Q15052
TMEM164	Q5U3C3	Q9H244	TMEM178A	Q8NBL3	Q12959
TMEM234	Q8WY98	Q8N130	TMEM255A	Q5JRV8	Q96J02
TMEM266	Q2M3C6	O60341	TMEM40	Q8WWA1	P13569
TMEM59	Q9BXS4	Q13332	TMPO	P42166	Q93009
TMPRSS12	Q86WS5	Q92521	TMUB2	Q71RG4	Q14973
TNFRSF14	Q92956	Q7Z6A9	TOE1	Q96GM8	O95149, P62306, P14678, P62304
TOP1	P11387	P00519	TPM1	P09493-10, P09493	Q9Y6D9
TPT1	P13693	P29692	TRAFD1	O14545	Q96RK4
TRIM14	Q14142	P61024	TRIM44	Q96DX7	Q3SYG4, Q9BCX9
TRIM71	Q2Q1W2	Q9H9Z2	TRIM9	Q9C026	P48730
TSPAN2	O60636	P17931	TSPAN3	O60637	Q9NPF0
TSPYL4	Q9UJ04	O00273	TTYH3	Q9C0H2	P21453

Input	UniProt Id	Interacts with	Input	UniProt Id	Interacts with
TUT1	Q9H6E5	P62306, P14678, P62304	TXK	P42681	O14543
UBE2D2	P62837	Q9Y4K3	UBE2F	Q969M7	P26367
UBE2V2	Q15819	Q14527, P61088	UBL5	Q9I9K6	P24864
UBXN7	O94888	Q9Y4K3	UGT1A8	Q9HAW9	P22309
UQCRH	P07919	P31930, Q9UDW1, O14949, P14927, P22695	URB1-AS1	Q96HZ7	P25788
USP16	Q9Y5T5	O95714	USP2	O75604	Q9Y4K3
USP21	Q9UHP3	Q9UKG9	USP27X	A6NNY8	Q96B97
USP44	Q9H0E7	P41208	USP47	Q96K76	P52198
VAX2	Q9UIW0	Q9Y3E7	VPS18	Q9P253	P0DTC3
VPS37A	Q8NEZ2	P54252	VRK2	Q86Y07-2, Q86Y07-1	Q13469
VSNL1	P62760	P04155	WBP1L	Q9NX94	Q8N2W9
WBP4	O75554	P62306	WDFY4	Q6ZS81-2	Q96CV9
WDR44	Q5JSH3	P16284	WDR77	Q9BQA1	P03418
WDR82	Q6UXN9	P36873	WDR83	Q9BRX9	O75695
WDTC1	Q8N5D0	Q13371	WFDC2	Q14508	P08253
WNK1	Q9H4A3	Q15149	XCL1	P47992	P13501, P48061
XPC	Q01831	P06746	XRCC4	Q13426	P19838
YWHAB	P31946	P49815	ZBTB17	Q13105	P04198
ZC2HC1B	Q5TFG8	O43639	ZC4H2	Q9NQZ6	P55040
ZDHHC9	Q9Y397	Q8WTR4	ZFYVE1	Q9HBF4	Q8NC69
ZMAT4	Q9H898-2	Q15633	ZMYND12	Q9H0C1	O60422
ZMYND8	Q9ULU4	P41182	ZNF23	P17027	Q13077
ZNF250	P15622-3	O75496	ZNF35	P13682	Q99836
ZNF398	Q8TD17	Q96CV9	ZNF479	Q96JC4	Q16623
ZNF484	Q5JVG2	Q13263	ZNF511	Q8NB15	Q9UI95
ZNF556	Q9HAH1	Q53H54	ZNF574	Q6ZN55	Q8TBF4
ZNF621	Q6ZSS3	P45973	ZNF622	Q969S3	Q6NZI2
ZNF627	Q7L945	Q04721	ZNF638	Q14966	Q9Y4Z2
ZNF764	Q96H86	Q8N2S1	ZSCAN1	Q8NBB4-2	Q00403
Input	ChEBI Id	Interacts with	Input	ChEBI Id	Interacts with
CFH	P08603	18132	RAB9A	P51151	15996
S100A13	P97352	29036			

## 7. Identifiers not found

These 888 identifiers were not found neither mapped to any entity in Reactome.

ADGRB2	ADORA2A-AS1	AFAP1L1	AGAP1	AGBL5-AS1	AGK-DT	ANKDD1B	ANKRD20A1
ANKRD35	ANP32C	AP3M2	APCDD1L-DT	AQP12B	ARHGAP11A-DT	ARHGAP11B-DT	ARHGEF35-AS1
ARHGEF38-IT1	ARMC2-AS1	ASAH2B	ATAD3C	ATE1-AS1	ATP8B1-AS1	B3GALT1-AS1	B4GALT4-AS1
B4GAT1-DT	BCL2L1-AS1	BIRC6-AS2	BLACAT1	BMPPR1B-DT	C10orf95	C12orf43	C17orf113
C19orf67	C20orf203	C2orf78	C4orf36	C5orf63	C6orf163	C8orf34-AS1	CACNA2D4
CADPS2	CALB2	CALML3-AS1	CARD16	CATIP-AS1	CCDC160	CCDC18-AS1	CCDC81
CDC20-DT	CDC42P3	CDH13-AS2	CDRT4	CEBPA-DT	CELF2-AS1	CENPVL2	CEP104
CEP295NL	CETN4P	CFAP119	CFAP20DC	CFAP61	CFAP69	CH507-145C22.1	CHMP3-AS1
CHRAC1	CLDN34	CLYBL-AS3	CMPK2	CNNM3-DT	CNTN4-AS2	CNTNAP3B	COL5A1-AS1
COX7B2	CPNE4	CRISP1	CRYM-AS1	CTAGE10P	CYP4F24P	DANT1	DAW1
DCDC1	DDX11L17	DIP2A-IT1	DLGAP4-AS1	DLK2	DNAI7	DNAJC3-DT	DNASE1L3
DNM1P35	DPY19L2	DQX1	DTX2P1-UPK3BP1-PMS2P11	ECI2-DT	EFR3A	EGFLAM	ELF3-AS1
ELN-AS1	ELOF1	ENPP5	EOLA1-DT	EPHX3	EPIC1	EPN2-IT1	ERICH6B
ERLNc1	ERV3-1	ERVV-1	ESPNP	ETDA	EXOC3L4	EXOSC10-AS1	F10-AS1
FAM193B-DT	FAM205A	FAM247D	FAM88C	FBXO8	FCGR2C	FEZF1-AS1	FGGY-DT
FHDC1	FIBIN	FJX1	FLJ30679	FLJ36000	FLJ42393	FNDC5	FOXP1-AS1
FREM3	FRG2C	FRMD4B	FSCB	FTO-IT1	FTX	GAL3ST4	GAS5
GBP1P1	GDNF-AS1	GIPC3	GLIPR1L1	GLIPR2	GOLGA6D	GOLGA8M	GPALPP1
GPR137C	GPR157	GPR34	GPR84-AS1	GREB1L-DT	GRIK1-AS2	GTDC1	GTF3C2-AS1
GTF3C2-AS2	GUSBP11	GYG2P1	Gene	H2BW3P	HCG26	HEATR5A-DT	HEPN1
HEXA-AS1	HFM1	HLA-DPB2	IFITM4P	IFITM5	IFRD1	IGHEP1	IGHVIII-38-1
IGSF21	IGSF9B	IMPG2	INA FM2	INKA2-AS1	INSM2	IPO5P1	ITGB2-AS1
KBTBD11	KCNK15-AS1	KCNMA1-AS3	KCNQ5-IT1	KHDC1	KIAA0513	KIZ-AS1	KLHDC7A
KLHL29	KRT16P1	KRT16P2	LBH	LDLR-AS1	LDLRAD2	LHFPL3	LINC00106
LINC00260	LINC00310	LINC00313	LINC00339	LINC00442	LINC00479	LINC00504	LINC00574
LINC00672	LINC01011	LINC01095	LINC01132	LINC01145	LINC01166	LINC01170	LINC01208
LINC01214	LINC01249	LINC01278	LINC01311	LINC01338	LINC01347	LINC01402	LINC01430
LINC01436	LINC01569	LINC01617	LINC01647	LINC01659	LINC01678	LINC01687	LINC01783
LINC01792	LINC01856	LINC01907	LINC01967	LINC02061	LINC02084	LINC02088	LINC02308
LINC02316	LINC02346	LINC02544	LINC02606	LINC02613	LINC02614	LINC02675	LINC02716
LINC02726	LINC02736	LINC02762	LINC02798	LINC02809	LINC02935	LINC02940	LINC02982
LINC02995	LINC03014	LINC03034	LIPE-AS1	LITAFD	LMLN	LOC100129617	LOC100132077
LOC100272217	LOC100287036	LOC100289511	LOC100505716	LOC100505728	LOC100505774	LOC100506405	LOC100506532
LOC100506851	LOC100506974	LOC100996379	LOC100996506	LOC100996842	LOC101927483	LOC101927511	LOC101927687
LOC101927825	LOC101927829	LOC101927872	LOC101927919	LOC101928008	LOC101928051	LOC101928279	LOC101928572
LOC101928701	LOC101928817	LOC101928842	LOC101928855	LOC101928957	LOC101929140	LOC101929240	LOC101929256
LOC101929534	LOC101929759	LOC101930091	LOC101930100	LOC102723409	LOC102723506	LOC102723544	LOC102723575
LOC102723665	LOC102723724	LOC102723733	LOC102723750	LOC102723758	LOC102723855	LOC102723872	LOC102724081
LOC102724093	LOC102724250	LOC102724370	LOC102724521	LOC102724587	LOC102724615	LOC102724748	LOC102724851
LOC102724877	LOC102725180	LOC105369308	LOC105369318	LOC105369460	LOC105369587	LOC105369625	LOC105369704
LOC105369719	LOC105369759	LOC105369869	LOC105369923	LOC105369999	LOC105370003	LOC105370027	LOC105370032
LOC105370035	LOC105370271	LOC105370314	LOC105370353	LOC105370364	LOC105370408	LOC105370436	LOC105370476

LOC105370492	LOC105370688	LOC105370897	LOC105370910	LOC105370921	LOC105370948	LOC105371081	LOC105371089
LOC105371103	LOC105371121	LOC105371159	LOC105371167	LOC105371172	LOC105371216	LOC105371217	LOC105371229
LOC105371289	LOC105371649	LOC105371686	LOC105371753	LOC105371761	LOC105371818	LOC105371976	LOC105372146
LOC105372158	LOC105372159	LOC105372345	LOC105372491	LOC105372505	LOC105372631	LOC105372661	LOC105372662
LOC105372816	LOC105372832	LOC105372842	LOC105372850	LOC105372862	LOC105372960	LOC105373043	LOC105373264
LOC105373311	LOC105373369	LOC105373387	LOC105373428	LOC105373447	LOC105373512	LOC105373527	LOC105373559
LOC105373598	LOC105373623	LOC105373760	LOC105373826	LOC105373938	LOC105373978	LOC105373994	LOC105374010
LOC105374024	LOC105374034	LOC105374071	LOC105374118	LOC105374122	LOC105374141	LOC105374147	LOC105374171
LOC105374246	LOC105374325	LOC105374339	LOC105374349	LOC105374355	LOC105374358	LOC105374478	LOC105374493
LOC105374524	LOC105374584	LOC105374775	LOC105374923	LOC105374925	LOC105374928	LOC105374953	LOC105374966
LOC105375012	LOC105375106	LOC105375130	LOC105375216	LOC105375228	LOC105375322	LOC105375387	LOC105375466
LOC105375497	LOC105375501	LOC105375536	LOC105375541	LOC105375543	LOC105375871	LOC105375921	LOC105375943
LOC105375980	LOC105375981	LOC105376011	LOC105376063	LOC105376127	LOC105376195	LOC105376235	LOC105376322
LOC105376447	LOC105376535	LOC105376536	LOC105376753	LOC105376786	LOC105376861	LOC105376963	LOC105377085
LOC105377258	LOC105377294	LOC105377320	LOC105377343	LOC105377358	LOC105377524	LOC105377763	LOC105377779
LOC105377891	LOC105378230	LOC105378551	LOC105378568	LOC105378626	LOC105378632	LOC105378675	LOC105378691
LOC105378717	LOC105378748	LOC105378758	LOC105378768	LOC105378779	LOC105378841	LOC105378973	LOC105379007
LOC105379021	LOC105379066	LOC105379087	LOC105379250	LOC105379251	LOC105379428	LOC105379453	LOC105379521
LOC105379524	LOC107984116	LOC107984150	LOC107984225	LOC107984254	LOC107984276	LOC107984302	LOC107984308
LOC107984352	LOC107984376	LOC107984407	LOC107984413	LOC107984444	LOC107984456	LOC107984469	LOC107984482
LOC107984485	LOC107984537	LOC107984583	LOC107984670	LOC107984788	LOC107984840	LOC107984910	LOC107984948
LOC107985019	LOC107985172	LOC107985286	LOC107985302	LOC107985317	LOC107985320	LOC107985414	LOC107985423
LOC107985522	LOC107985568	LOC107985594	LOC107985675	LOC107985700	LOC107985897	LOC107985898	LOC107985940
LOC107985986	LOC107986024	LOC107986073	LOC107986079	LOC107986080	LOC107986129	LOC107986162	LOC107986254
LOC107986260	LOC107986334	LOC107986424	LOC107986434	LOC107986477	LOC107986489	LOC107986543	LOC107986571
LOC107986800	LOC107986909	LOC107986910	LOC107986918	LOC107986973	LOC107986981	LOC107986991	LOC107987006
LOC107987010	LOC107987071	LOC107987073	LOC107987076	LOC107987101	LOC107987145	LOC107987220	LOC107987221
LOC107987258	LOC107987262	LOC107987290	LOC107987304	LOC107987324	LOC107987338	LOC107987348	LOC107987363
LOC107987374	LOC107987388	LOC112267907	LOC112267930	LOC112267942	LOC112267986	LOC112268035	LOC112268047
LOC112268077	LOC112268104	LOC112268148	LOC112268166	LOC112268205	LOC112268227	LOC112268418	LOC112268421
LOC112268423	LOC112268446	LOC114224	LOC151760	LOC153910	LOC283045	LOC339666	LOC339975
LOC388242	LOC388436	LOC389906	LOC392364	LOC401127	LOC441081	LOC646548	LOC731075
LPEQ6126	LPGAT1-AS1	LRRC19	LRRN4CL	LY75-CD302	LYPLAL1-AS1	MAGEA5P	MAGEB5
MAGOH-DT	MAP2K4P1	MAPT-IT1	MASCRNA	MATCAP1	MBD3L2B	MBD3L5	MBNL1-AS1
MBNL2	ME3-DT	MEF2C-AS1	MFSD4B-DT	MIDEAS-AS1	MIR10392	MIR103B2	MIR1206
MIR1225	MIR1226	MIR1238	MIR1302-9	MIR1909	MIR198	MIR3178	MIR3188
MIR3605	MIR3613	MIR3614	MIR3926-2	MIR4257	MIR4290	MIR4291	MIR4292
MIR4293	MIR4295	MIR4298	MIR4299	MIR4300	MIR4304	MIR4308	MIR4489
MIR4516	MIR4741	MIR499B	MIR5001	MIR555	MIR6084	MIR6511B1	MIR657
MIR6752	MIR6753	MIR6757	MIR6784	MIR6797	MIR6811	MIR6822	MIR6836
MIR6848	MIR6873	MIR6882	MIR7113	MIR762	MIRLET7BHG	MIRLET7E	MIRLET7F1
MIRLET7F2	MIRLET7I	MISFA	MISP3	MIX23	MKLN1-AS	MKRN7P	MKRN9P
MKX-AS1	MRPL45P2	MSANTD2-AS1	MSC-AS1	MSRA-DT	MTX3	MYCBP	MYRF
NAALADL2-AS3	NBPF15	NDRG3	NDUFA4L2	NDUFB2-AS1	NEXMIF	NF1P2	NGFR-AS1
NPIPA5	NPTN-IT1	NSUN7	NXT1-AS1	P3R3URF-PIK3R3	PAN3-AS1	PARD3-DT	PATE2
PAXBP1-AS1	PAXIP1-DT	PCCA-DT	PCDHA1	PCDHA7	PCDHB12	PCDHB6	PCDHB9
PCNX4-DT	PCOLCE-AS1	PCP4L1	PDCD4-AS1	PDCD6P1	PDK4-AS1	PFN1P2	PFN3
PICART1	PITPNA-AS1	PKD1-AS1	PKD1L2	PKD1P6-NPIPP1	PLD5	PNKY	POLR2J4

PP2D1	PPM1K-DT	PPP1R42	PPP4R1L	PPP4R3B-DT	PRAMEF2	PRAMEF6	PRAMEF7
PRAMEF8	PRAMEF9	PRCD	PRICKLE4	PRKAG2-AS1	PRORY	PVRIG2P	PWWP3A
PXK	RAB5C-AS1	RABGEF1P1	RALGPS1	RASSF9	RAVER2	RBFADN	RFPL4A
RHOQ-AS1	RN7SK	RN7SL832P	RNA28SN4	RNA5-8SN1	RNA5-8SN2	RNASE4	RNF207-AS1
RNF222	RPL17-C18orf32	RPL34-DT	RPSA2	RSPH4A	SACS-AS1	SAMD5	SCARNA17
SCARNA21	SCARNA7	SCART1	SCGB1B2P	SCHLAP1	SDAD1-AS1	SEMA3F-AS1	SEPTIN4-AS1
SEPTIN7P2	SEZ6	SGSM3-AS1	SH3BP5-AS1	SHISA2	SIDT1	SKA3	SLC22A14
SLC38A4-AS1	SLC49A3	SLC7A6OS	SLTM	SMARCA5-AS1	SMCO2	SMCR5	SNHG18
SNHG22	SNHG7	SNORA103	SNORA28	SNORA30	SNORA33	SNORA3B	SNORA47
SNORA53	SNORA58B	SNORA9	SNORA9B	SNORD116-13	SNORD136	SNORD13C	SNORD150
SNORD19C	SNORD25	SNORD35B	SNORD3K	SNORD41	SNORD49A	SNORD50A	SNORD54
SNORD56	SNORD69	SNORD72	SNORD79	SNORD89	SNRK-AS1	SPAG16-DT	SPDYE14
SPDYE15	SPECC1L-ADORA2A	SPINK8	SPRNP1	SRP14-DT	SSBP3-AS1	ST20-AS1	STARD7-AS1
STAU2-AS1	STEAP1B	STEAP3-AS1	SWINGN	TAPT1-AS1	TARS1-DT	TBC1D22A-AS1	TBC1D3K
TBC1D8-AS1	TBX2-AS1	TBX3-AS1	TERB1	THAP9	THORLNC	TLCD5	TMEM123-DT
TMEM217	TMEM235	TMEM238L	TMEM59L	TMEM72-AS1	TP53I11	TP53INP2	TPI1P2
TPSG1	TRA-TGC5-1	TRC-GCA23-1	TRC-GCA7-1	TRE-TTC4-2	TRH-GTG1-6	TRK-TTT3-5	TRL-CAG2-1
TRM-CAT3-1	TRM-CAT6-1	TRN-GTT25-1	TRNP1	TRP-TGG3-2	TRQ-CTG6-1	TRR-CCT4-1	TRV-TAC3-1
TSL	TSPAN13	TSPY8	TTTY6	TYRO3P	VSTM5	WDPCP	WDR47
WEE2-AS1	WHAMMP2	XPC-AS1	ZBBX	ZBTB7C-AS1	ZCCHC24	ZDHHC4	ZFAND3-DT
ZFHX4-AS1	ZNF137P	ZNF213-AS1	ZNF271P	ZNF321P	ZNF516-AS1	ZNF528-AS1	ZSWIM1